Mechanisms of the regulation of apoptosis

A Senior Honors Thesis

Presented in Partial Fulfilment of the Requirements for graduation
with research distinction in Molecular Genetics in the undergraduate colleges
of The Ohio State University

By
Janet M. Doolittle

The Ohio State University
May 2008

Project Adviser: Assistant Professor Andrea Doseff, Department of Molecular Genetics, Department of Internal Medicine

Abstract

Apoptosis, or programmed cell death, is an evolutionarily conserved developmental program that determines cell fate and acts as a defence mechanism, eliminating pathogen-infected cells and cells that have accumulated undesirable mutations. Misregulation of apoptosis has been implicated in a number of diseases, making knowledge of the mechanisms that dictate its execution of great importance to human health. Cell death is accomplished by a family of proteases known as caspases, and has recently been shown to be influenced by protein kinase Cδ (PKCδ) through its ability to phosphorylate caspase-3.

In order to study the mechanisms of apoptosis, a multidisciplinary approach was employed. First, a simplified mathematical model was created to describe the molecular interactions of PKCδ with caspase-3 and expanded to study the mechanisms of the flavonoid apigenin in inducing apoptosis. The model predicts a threshold condition for the activation of caspase-3 and also corroborates biological experiments showing caspase-3 activation prior to caspase-9. In addition, our mathematical model predicted that PKCδ reaches a threshold apoptotic level in apigenin-induced apoptosis. These findings were experimentally validated using a biological system. To further investigate the means by which apigenin induces apoptosis, we used a microarray of leukemia cells treated with apigenin to identify genes that may be transcriptionally regulated by apigenin. We also expanded the investigation into caspase-3 phosphorylation by examining the structure of six sites mapped by mass spectrometry. The evolutionary conservation and accessibility of each site was considered. Single and multiple site-directed mutagenesis was performed to create phosphomimicking mutations at the sites in question. The enzyme activity of caspase-3 phospho mutants was determined using purified proteins.

Thus, we have investigated means of regulating caspase-3 activity, using PKCδ and apigenin as instruments of cell death. We developed a model of the PKCδ-caspase-3 relationship and explored the structural constraints involved. The more that is known about the mechanisms by which apoptosis functions and malfunctions, the better we will be able to exploit this knowledge to develop new treatments for the array of human diseases caused by deregulated apoptosis.

Introduction

Apoptosis is a highly regulated developmental program in which several signalling cascades converge to trigger a series of biochemical and morphological changes within a cell, leading to its death. This course of action, when executed at appropriate times, is important for not only for development, but also to protect the body from cells that have accumulated mutations or been infected by pathogens. Thus, proper regulation of apoptosis is essential to keep the homeostatic cellular balance. However, when misregulated, apoptosis can contribute to disease. Excessive apoptosis of neurons due to toxic protein aggregates and oxidative stress has been implicated in Alzheimer and Parkinson's diseases, whereas failure to execute apoptosis contributes to atherosclerosis, chronic inflammation, and cancer (1, 2, 3, 4).

Apoptosis can be activated by several apoptotic cascades that involve the caspases, a family of evolutionarily conserved cysteine proteases (Figure 1) (5, 6). Caspases can be classified into initiator and effector caspases based on their role in the apoptotic cascade. Initiator caspases, such as caspase-8 and caspase-9, are activated by autocatalytic cleavage in response to the instigation of apoptosis. The activation of the effector caspases, such as caspase-3, caspase-6, and caspase-7, is dependent on proteolysis by an initiator caspase (7). The extrinsic pathway of apoptosis is initiated when a death domain (DD) containing member of the tumor necrosis factor (TNF) receptor superfamily, such as Fas or TRAIL, is activated by the binding of a specific extracellular ligand. The death receptor recruits proteins to form the Death Inducing Signalling Complex (DISC), which activates caspase-8 (8). The intrinsic pathway is activated by radiation or by chemotherapeutic drugs. In this apoptotic pathway, changes within the cell result in mitochondrial depolarization and release of cytochrome c into the cytoplasm. Cytochrome c binds to Apaf-1 and these two cofactors enable activation of caspase-9 (Figure 1) (7, 9).

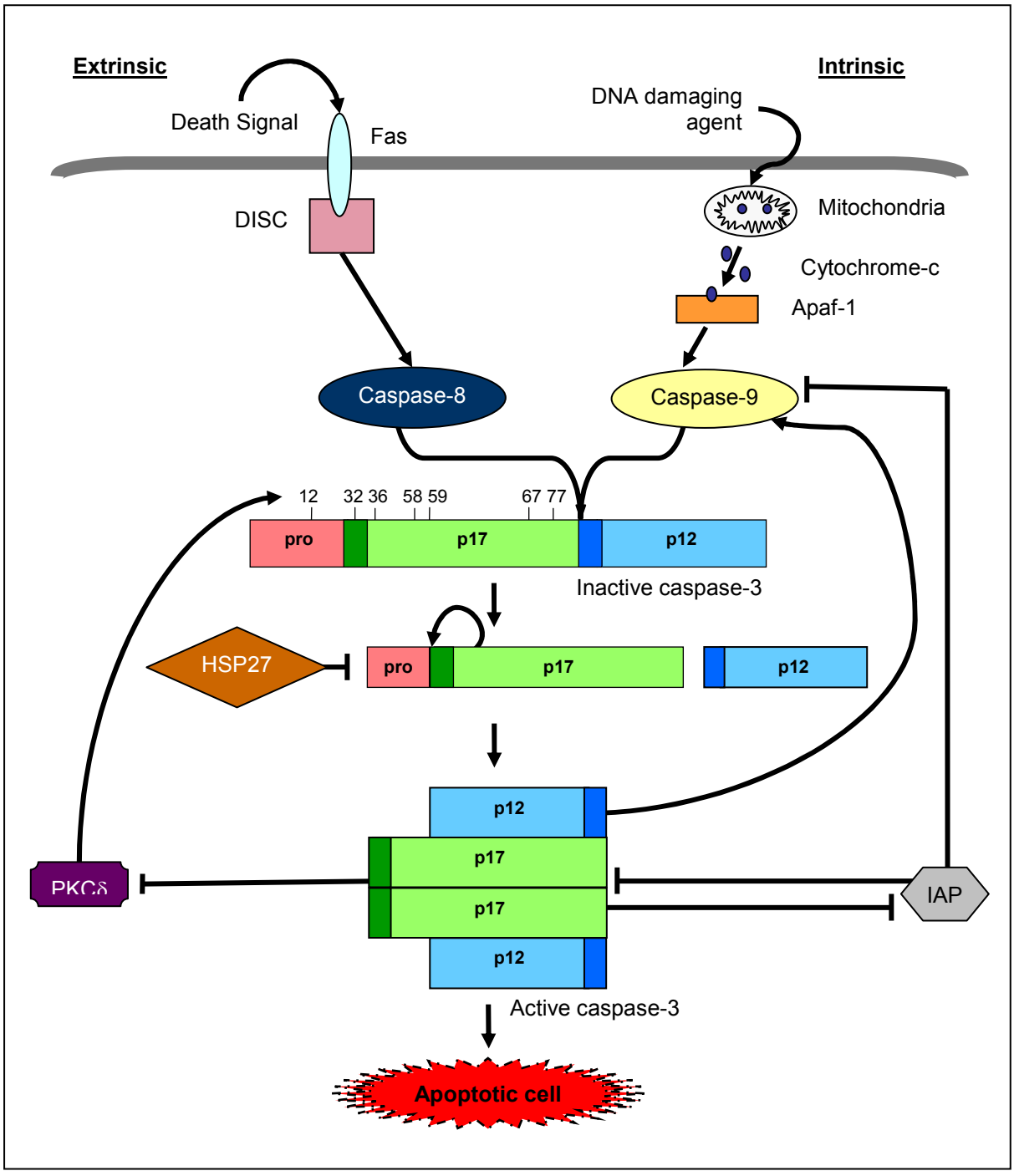

Figure 1- Simplified model of the apoptotic cascade.

Caspase-3 is a central effector caspase that can be activated through either the extrinsic and intrinsic signalling cascades involving the initiator caspases, caspase-8 and

caspase-9, respectively (Figure 1) (10, 11). Caspases-6 and -7, other effector caspases with similar structures to that of caspase-3, can also be activated during this cascade (12). Caspase-3 is synthesized as an inactive precursor which consists of three domains, the N-terminal prodomain, the p12 domain, and the C-terminal p17 domain (13). Once an initiator caspase has been activated, it performs the first of two sequential cleavages required to activate caspase-3, between the p17 and p12 domains (10). The second cleavage, between the pro and p17 domains, is autocatalytic an enables the formation active caspase-3, a tetramer consisting of two p17 and two p12 domains arranged head to tail (Figure 1) (14, 10, 15).

Once active, caspase-3 mediates the proteolysis of several proteins with diverse biological functions, including, among others, molecules involved in chromatin assembly, transcription factors, and modulators of signal transduction pathways (16) (Figure 1). Cleavage of caspase-3 substrates causes morphological changes including chromatin condensation, nuclear fragmentation, and membrane blebbing which result in the formation of an apoptotic body. Apoptotic bodies prevent damage to surrounding cells by confining the contents of the dying cell until it can be phagocytized by a macrophage (7, 10). Activated caspase-3 has been shown to participate in positive feedback cleavage of caspase-9, which is necessary to fully activate caspase-9 during staurosporine-induced apoptosis in mouse embryos and with purified human recombinant proteins *in vitro* (17, 18) (Figure 1).

The molecular pathways regulating apoptosis are increasingly revealed, giving a very complex, but still incomplete, picture of how cell fate is determined. Since the activation of caspase-3 is the central step in the execution of apoptosis, a better understanding of its regulation will provide the invaluable potential to modulate cell fate at will. Interestingly, while much is known about the regulators of initiator caspases such as caspase-9, or -8, little is known about the regulators of caspase-3 (6). One family of proteins that has a role in

regulating apoptosis is the BCL2 family. BCL2 family proteins play opposing roles in apoptosis, with anti-apoptotic members like BCL2 and BCL-XL and pro-apoptotic members such as Bax and Bak. Their role is mostly upstream of caspase-3, by regulating changes in the mitochondria, which can lead to apoptosis (19). Another family, the inhibitor of apoptosis proteins (IAP) family, plays a more direct role in caspase regulation. Members of the IAP family, including XIAP, c-IAP1, and c-IAP2, were shown to associate directly with the active forms of caspase-3, caspase-7, and caspase-9, inhibiting their activities (9, 20). All IAP proteins contain a baculovirus IAP repeat (BIR) domain, and several also contain a RING domain. The RING domain has E3 ubiquitin ligase activity and XIAP has been shown to mediate proteasomal degradation of caspase-3 (9, 21). XIAP, the most extensively studied member of the IAP family, binds caspase-3 and caspase-7 in a manner that covers the active site of the protease and prevents substrates from binding. XIAP binds the small subunit of caspase-9 only after the recognition site is revealed by cleavage of caspase-9. In contrast to its binding to caspase-3, it is unclear whether or not this interaction blocks the active site of capsase-9, so the mechanism by which XIAP inhibits caspase-9 is unknown (9). Notably, XIAP can be cleaved by active caspase-3 resulting in the inactivation of its inhibitory function (Figure 1) (22). In contrast to the IAPs, small heat shock protein 27 (Hsp27), another protein that is able to regulate caspase-3 by direct binding, binds to the pro domain of inactive caspase-3 and prevents the second cleavage that is needed for activation (Figure 1). Hsp27 is constitutively expressed in monocytes, but relocalizes to the nucleus during spontaneous apoptosis. Consistent with its role as an inhibitor of caspase-3, it was shown that RNA interference against Hsp27 induces apoptosis in monocytes, while overexpression of Hsp27 lengthens monocyte life span (23).

Another recently discovered specific direct regulator of capsase-3 is Protein Kinase Cδ (PKCδ) (24). The PKC family of serine/threonine kinases has many isoforms, some of

which are pro-apoptotic, including PKCδ, and others that are anti-apoptotic (25). PKCδ is classified as a novel PKC because its activation can be induced by DAG and PMA, but is independent of Ca^{2+}, unlike the conventional PKCs which do respond to Ca^{2+} and the atypical PKCs which respond to neither DAG nor Ca^{2+} but are activated by phorbol esther. PKCδ is known to phosphorylate a number of substrates including proteins involved in translation, such as eukaryotic elongation factor 1-α (eEF-1α) and mTOR, as well as several transcription factors, including Sp1, NFκB, and STAT1 (26). Upon activation, PKCδ translocates from the cytoplasm to the plasma membrane. PKCδ associates with and phosphorylates caspase-3, contributing to its apoptotic activity. During apoptosis, active caspase-3 induces the cleavage of PKCδ, causing the catalytic domain of PKCδ to translocate to the nucleus where it can phosphorylate a different subset of cellular targets (26, 27) (Figure 1). The activation of PKCδ has also been seen during the induction of apoptosis by several known anti-cancer agents (28, 29, 30). Thus, caspase-3 can be regulated at multiple checkpoints, creating a safety-lock during the normal cellular life span. Caspase-3 regulation has been demonstrated to occur by a variety of mechanisms and at several different stages during the process of activation, adding complexity to the study of caspase-3 regulation.

The problem of conventional anti-cancer treatments failing due to malignant cells acquiring multi-drug resistance has prompted the identification and understanding of alternative compounds that induce cell death. However, while these compounds are being identified rapidly, understanding their mechanisms of action is a time consuming process and in the majority of cases, remains to be elucidated (7). Apigenin is a plant polyphenolic compound found in fruits and vegetables like parsley, onions, tea, citrus fruits, red wine, and chamomile (31, 32), and is emerging as a potential anti-inflammatory, anti-oxidant, and anti-cancer compound (33, 34, 32, 35, 36). Using a human leukemia cell line, we recently demonstrated that PKCδ and caspase-3 activation mediate apoptosis induced by the flavonoid

apigenin (37). Apigenin inhibits the proliferation of several cancer cells with different potency (38, 39, 31). Notably, we found that apigenin is very effective in inducing apoptosis in leukemia cells (37). However, the mechanism by which apigenin acts is unclear. Studies in prostate or breast cancer have suggested a range of processes that apigenin may effect, including estrogen receptor β signalling (40), the NFκB cascade (41), the PI3K/AKT dependent ErbB2 pathway (31), the intrinsic pathway of apoptosis (42, 43), and the cell cycle (44).

Interestingly, defective activation of the apoptotic pathway has been found in some cancer cells, despite the fact that they express normal levels of caspase-3 and caspase-9 (45). These findings suggest the existence of additional mechanisms involved in the activation of the caspases that might be impaired in cancer cells, halting the ability of cancer drugs to trigger apoptosis. In this context, the loss of the PKCδ activity, a positive regulator of caspase-3, has been reported in breast cancer epithelial cells (46). Furthermore, decreased expression of PKCδ increased tumor production (47).

A multidisciplinary approach was taken to aid in understanding the complex regulation of caspase-3. First, a simplified mathematical model was created to describe the molecular interactions of PKCδ with caspase-3. Simulations of caspase-3 and caspase-9 activities were validated by comparison to biological results obtained with leukemia cells treated with etoposide. The model was expanded to include the drug apigenin, in order to elucidate its mechanism of action. Using this *in silico* approach, we were able to reproduce major features of time-series experiments on PKCδ and caspase-3 activities obtained using chemotherapeutic-induced-apoptosis. Conditions predicted by the model for the promotion of apoptosis were then corroborated using a biological system. Model predictions include the requirement of a minimum amount of PKCδ for the induction of caspase-3 activation. The model also vindicates experiments that showed the possibility that under certain

circumstances caspase-3 activity prior to caspase-9. Although this aspect was not discussed, data from some groups shows that caspase-3 activity begins to increase before caspase-9 activity during apoptosis induced by a variety of agents, including apigenin and UV (37, 48). Moreover, based on our predictions, we conducted experiments to confirm the minimum level of PKCδ activity required to reach an apoptotic threshold in apigenin treated cells. In addition, a microarray approach was used to identify genes in a leukemia cell line that may be differentially expressed in response to apigenin treatment.

The importance of PKCδ in the regulation of caspase-3-dependent apoptosis compelled us to investigate the mechanism of caspase-3 phosphorylation. For this purpose, we determined the caspase-3 phosphorylation sites using *in silico* approaches and mass spectrometry and used structural analysis to examine six of these sites in more detail. The structure of four sites was found to be evolutionarily conserved in mammals, and the accessibility of each of these sites was assessed. Single and multiple site-directed mutagenesis was performed to create phosphomimicking mutations at the sites in question. The ability of the caspase-3 phospho mutants to cleave a specific peptide substrate was determined using purified proteins.

Thus, we have developed a model of the PKCδ-caspase-3 relationship and explored the structural constraints involved. The model predicted that activation of PKCδ is necessary for caspase-3 activation in apigenin-induced-apoptosis and that a threshold of apigenin can activate PKCδ. Importantly, we were able to validate this latter result using *in vitro* kinase assays in cells undergoing apoptosis and experiments to identify PKCδ-dependent phosphorylation sites are underway. Understanding the mechanisms that dictate cell death will aid in developing treatments for the numerous diseases caused by deregulated apoptosis.

Materials and Methods

The mathematical model

Construction of the model

The construction of the "Caspase-3 Regulation" model was guided by known interactions between the elements of the model found in the literature (Table 2, at end of text). The model contains the intrinsic pathway of apoptosis, with the addition of interactions involving PKCδ and a positive feedback loop between caspase-9 and caspase-3 (49). In order to maintain simplicity, the interactions upstream of caspase-9 were condensed into a single step referred to as "Upstream Elements" in the model. In this way, we maintain simplicity without ignoring many important interactions in the intrinsic pathway. Similarly, while there are a number of inhibitors of apoptosis proteins, including XIAP, c-IAP1, and c-IAP2, the combined influence of these proteins is represented in the model simply by "IAP." Ordinary differential equations were used to describe the behaviour of each species in the model.

The model was translated into computer code and simulated using the software Berkeley Madonna version 8.3.9 (R. Macey and G. Oster, University of California at Berkeley). The simulations were carried out using the Runge-Kutta 4 integration method. The resulting data were saved in table format, and graphed in Excel for aesthetic purposes.

For the determination of thresholds and prediction of PKCδ activity, the model was altered so that k_{3a} and apigenin, respectively, would be treated as variables, rather than parameters. To do this, these values were removed from the list of parameters and given an initial value of 0 and a differential equation in which they increased at a constant rate. To add apigenin to the model, the equation for v_3 was altered to include the effect of apigenin on

PKCδ activation (See supplementary material 1: Model code for the equations used for each version of the model).

Legitimizing parameters and using the model to make predictions

In addition to a qualitative comparison of the model with experimental data, the values of the parameters used in the simulations were checked against known parameters. The literature was searched to find values for the rate constants used in the model, and these values are shown in Table 2. In the model, the parameters are values that have arbitrary units with no biological meaning. To compare parameters with arbitrary units to known values, the rate equations were rewritten so that all of the units cancelled out. The resulting dimensionless equations are shown in supplementary material 3: Dimensionless equations. These equations contain unit-less parameters that are equal to ratios of rate constants [for example: $h_7 = (k_7) / (K_{m1a}*k_{-7}) =$ (concentration/time) / (concentration/time)]. The unit-less parameters are in supplementary material 4: Parameter values, along with the values of their ratio in both the simulations and the literature. The model parameters were altered within an acceptable range around the literature values in order to make predictions about the behaviour of the system.

Cell culture and reagents

THP-1 cells were grown at 37°C in a humidified atmosphere of 95% air and 5% CO_2 in media supplemented with 100 U/ml penicillin, and 100 mg/ml streptomycin (BioWhittaker, Walkersville, MD). THP-1 cells were maintained in RPMI 1640 medium with L-glutamine (BioWhittaker, Walkersville, MD) supplemented with 5% fetal bovine serum (FBS, Hyclone, Logan, UT). Apigenin, etoposide, and the diluent dimethyl sulfoxide (DMSO) were obtained from Sigma-Aldrich (St. Louis, MO).

Caspase activity assays

Lysates from 3 x10^6 cells were prepared and incubated in a cytobuffer as previously described (37). The activity of caspase-3 was determined using the DEVD-AFC substrate and LEHD-AFC was used for caspase-9. Released AFC were measured using a Cytofluor 400 fluorimeter (Filters: excitation 400 nm, emission 508 nm; Perspective Co., Framingham, MA).

Immunoprecipitation and in vitro kinase assay

Extract preparation and immunoprecipitation with anti-PKCδ antibodies were carried out as previously described (24). After immunoprecipitation, kinase assays were performed by incubating protein A-loaded beads for 1 h at 37°C in the presence of 20 μl kinase assay buffer (25 mM Hepes pH 7.3, 10 mM $MnCl_2$, 1 mM $MgCl_2$, 1 mM DTT) containing 5 mCi of {γ^{32}P} ATP (Perkin Elmer, Boston, MA), 0.5 mM ATP. To each reaction, 5 mg of histone H2B (Boehringer Mannheim, Roche, Indianapolis, IN) was added as exogenous substrate. Reactions were stopped by the addition of 10 ml of 5X Laemmli buffer. Samples were boiled for 5 min and loaded onto a SDS-PAGE. The kinase activity was measured by PhosphorImager. The same membrane was immunoblotted with anti-PKCδ antibody to ensure equal loading of the samples.

The microarray

RNA isolation and microarray

THP-1 cells were cultured as above and either left untreated or treated with 50 μM apigenin for 3 h. Total RNA was purified from the cells using RNeasy Mini Kit (Qiagen, Valencia, CA). Hybridization of RNA to an Affymetrix Human Genome U133 Plus 2.0

Array (Affymetrix, Santa Clara, CA) was performed by the Functional Genomics Core at The Research Institute at Nationwide Children's Hospital (Columbus, OH).

Data analysis

Fold change was calculated for each gene, defined as the expression in the apigenin treated sample divided by the expression in the non-treated sample. Normalization, filtering, and data analysis was conducting using the software dChip (50). The data was filtered to find genes with a variation across samples of 1<std dev/mean<1000. Genes involved in biological processes of interest were identified in the list of filtered genes by hand and by comparison to Kyoto Encylopedia of Genes and Genomes (KEGG) (51, 52, 53) pathways of interest and using GenMapp mapps (54). Functions and roles of genes were investigated first by GO ((55) accessed May 17, 2007), then in more detail by literature search. The software GenMapp (54) was also used to identify genes of interest and generate images of pathways.

Phosphorylation mutants

Site-directed mutagenesis and cloning

Phosphosite mutants were generated with either alanine or aspartic acid in place of the wild type amino acid and a His_6 tag. Mutagenesis was conducted using Quick Change Single or Multi Site Directed Mutagenesis Kit (Stratagene, Cedar Creek, TX). Dpn1 treated DNA was transformed into *E. coli* M15 or XL1 Gold cells using the expression vector pQE31. Clones were screened by sequencing and analysis of inserts in a 1% agarose gel with 0.5 μg/mL ethidium bromide. Plasmid DNA was extracted from overnight cultures of Top10 F cells using a QIAprep Spin Miniprep Kit (Qiagen, Valencia, CA, cat.# 27106) and digested with SacI and XhoI to yield an insert of approximately 850 bp.

Protein purification

Bacteria was grown in Terrific Broth with appropriate antibiotics for selection to an OD of approximately A_{550} 0.5. Protein expression was induced with 1 mM isopropyl 1-thio-β-D-galactopyranoside (IPTG) for 30 minutes at 20°C. Bacteria were lysed by sonication in sonication buffer (50 mM sodium phosphate, pH 7.8, 300 mM NaCl, 5 mM β-mercaptoethanol, 1% Tween 20, and protease inhibitors (2 μg/ml chymostatin, pepstatin, leupeptin, antipain, and 1 mM PMSF)). Lysates were allowed to bind to Ni^{2+} beads (Qiagen, Valencia, CA) in the presence of RNase (5 μg/ml) for 2 h at 4 °C. The beads consist of nitrilotriacetic acid (NTA), a metal chelator that stably binds Ni^{2+}. The Ni^{2+} has two remaining ligand binding sites that it uses to bind histidine (Qiagen). The Ni^{2+} binds to the tag of 6 consecutive histidines on the protein, detaining the recombinant protein but allowing other proteins to flow through the column (Figure 2, A). Tween 20 in the buffer helps to prevent non-specific protein binding to the beads. After binding, the beads were washed with 16 ml of the buffer containing 50 mM HEPES, pH 7.4, 50 mM NaCl, 10% glycerol, 1% Tween 20, and 1 mM PMSF. The protein was eluted with 1-ml aliquots of a step gradient of imidazole dissolved in the wash buffer. The structure of imidazole is the same as the ring on histidine (Figure 2, B and C). Therefore, at high concentrations, imidazole competes with histidine for Ni^{2+} binding and causes the recombinant protein to be released from the beads (Qiagen). Elution fractions containing rCaspase-3 were identified by SDS-PAGE. The protein was dialyzed to dilute the imidazole and Tween 20, which could interfere with caspase-3 activity in later assays, and put the protein in a buffer that would allow for further chemical analysis. The dialysis buffer consisted of against 50 mM HEPES, pH 7.4, 50 mM NaCl, 10% sucrose, 5 mM DTT, with 1 L of buffer used for two 1 mL samples. Dialysis was performed for 6 h, changing to fresh buffer after 3 h, at 4°C and proteins were analyzed by Western Blot.

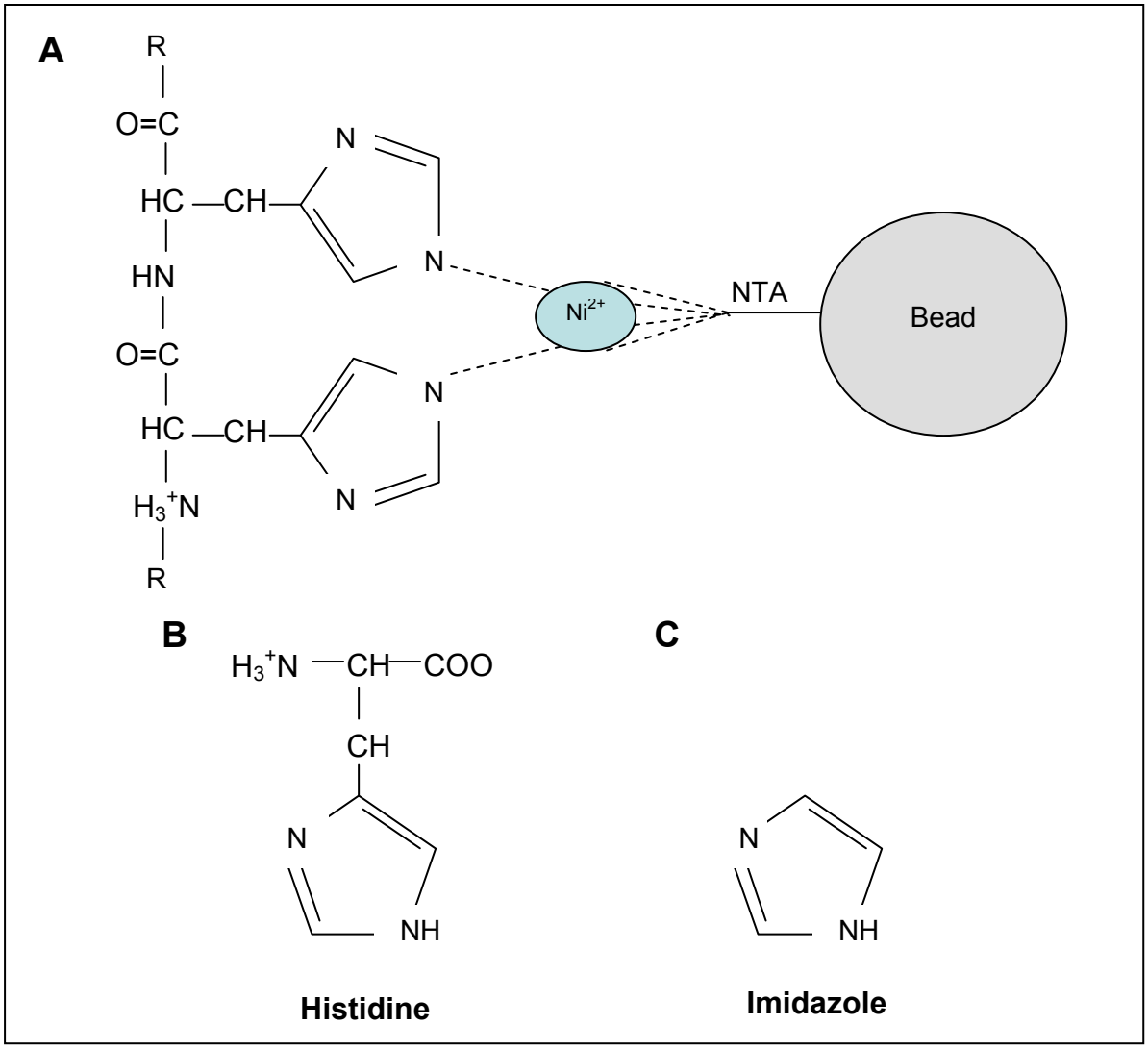

Figure 2- Structure of molecules involved in protein purification.
(A) Structure of His tag on recombinant protein bound to a bead through Ni^{2+}-NTA. (B) Structure of histidine. (C) Structure of imidazole. Adapted from Qiagen, The QIA*expressionist*, fifth edition.

Protein structure

Phosphorylation sites on caspase-3 were mapped by mass spectrometry. Potential phosphorylation sites were first investigated using the online phospho site prediction tools Motif Scan ((56), http://scansite.mit.edu/motifscan_seq.phtml), NetPhos (v. 2.0) and NetPhosK (v. 1.0) ((57) http://www.cbs.dtu.dk/services/NetPhos/, (58) http://www.cbs.dtu.dk/services/NetPhosK/), and Group-based Phosphorylation Scoring Method (GPS) (v. 1.10) ((59, 60) http://bioinformatics.lcd-ustc.org/gps_web/predict.php). A multiple alignment of caspase-3 from a variety of organisms was created using ClustalW and

used to asses the evolutionary sequence conservation of each site predicted by the online tools.

Protein structures were predicted using Swiss-Model in first approach mode (61, 62, 63, 64, 65). Structures were viewed and analyzed in DeepView Swiss-Pdb Viewer (http://www.expasy.org/spdbv/) (64). PyMolWin was also used to view structures and create movies (66).

Results

Development of the 'Caspase-3 Regulation Model'

Caspase-3 activation is very tightly controlled, requiring two sequential cleavages and phosphorylation, and sits at the crux of multiple apoptotic pathways, making the mechanism of its regulation exceptionally complex. To gain a better understanding of the regulation of apoptosis, we created a model of the intrinsic pathway of apoptosis by synthesizing previously published information on biological regulators of cell death and incorporating it into a mathematical description. This type of approach has been used previously to describe the biological behaviour of several signalling pathways, such as the NFκB pathway and the MAPK pathway (67, 68). We decided to concentrate on caspase-3 regulation due to its crucial role as a converging point for apoptotic signals and as an executioner of cell death and we included caspase-9 due to its relevance in chemotherapy-induced-apoptosis. (Figure 3, A, (9)). Biochemically, the initiator caspase-9 activates caspase-3 by inducing the first cleavage of caspase-3, which is followed by a second activating autocatalytic cleavage (Figure 3, B and C, (10, 69)). In turn, caspase-9 activity has been demonstrated to increase due to a positive feedback loop mediated by active caspase-3 (Figure 3, D and (17, 18)). Inactivation of both caspase-3 and caspase-9 is mediated at least in part by their ubiquitination by inhibitor of apoptosis proteins (IAPs) (Figure 3, E and (20, 21)). Caspase-3-dependent-cleavage of the IAPs impairs their inhibitory effect, prompting the execution of cell death (Figure 3, F and (22)). PKCδ, also included in the model, is a recently identified positive regulator of caspase-3, promoting its activation (Figure 3, G and (24)). Caspase-3 has been shown to cleave PKCδ, causing the relocalization of the cleaved PKCδ to the nucleus (Figure 3, H and (27)). We introduced inactive and cleaved PKCδ in the model as one entity, because neither is involved in the activation of caspase-3.

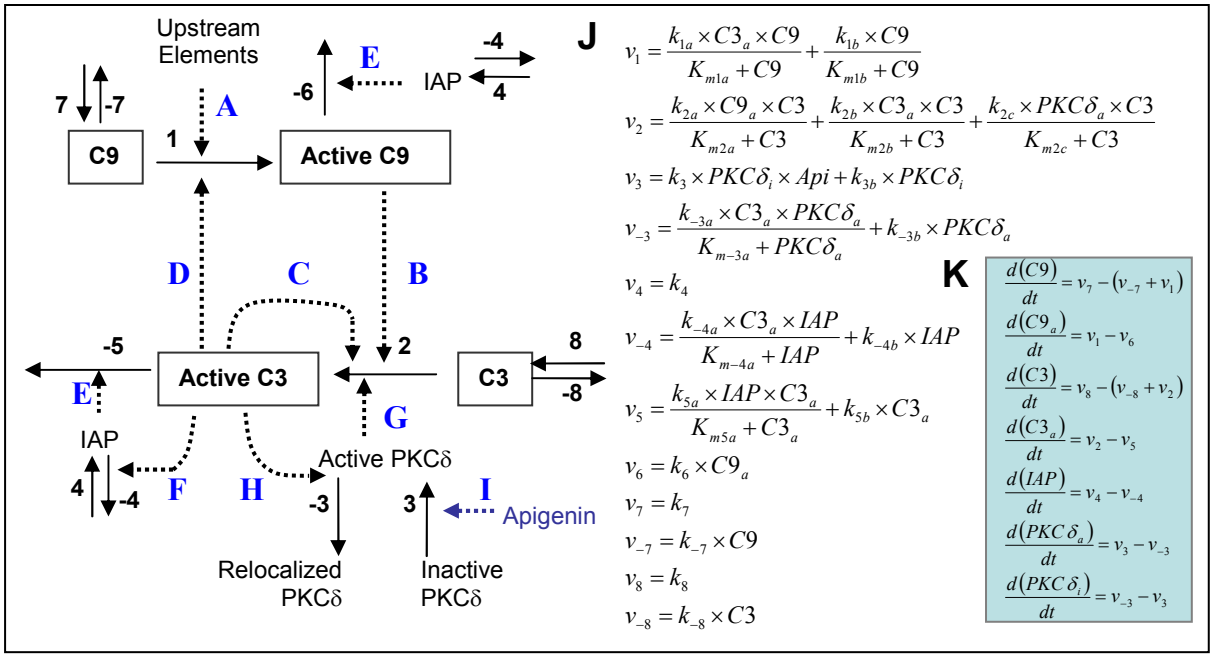

Figure 3 - Model of the intrinsic pathway of apoptosis.
(A) Upstream elements of the intrinsic pathway activate caspase-9. (B) Caspase-3 is activated by caspase-9 cleavage. (C) An autocatalytic cleavage also contributes to caspase-3 activation. (D) Active caspase-3 is involved in a positive feedback loop that activates caspase-9. (E) Active caspase-3 and active caspases-9 are ubiquitinated by IAP. (F) Active caspase-3 degrades IAP. (G) Caspase-3 activity is enhanced by phosphorylation by PKCδ. (H) Active caspase-3 is involved in a negative feedback loop with PKCδ. Caspase-3 cleaves PKCδ, causing it to translocate to the nucleus. (I) To study the effects of apigenin, it was added to some versions of the model (blue). Apigenin activates PKCδ. Solid arrows represent protein changing states by being either synthesized, activated, or degraded. Dashed arrows represent proteins that act as catalysts to promote a reaction. The numbers near the arrows are used to identify the rate reactions in (J), i.e. arrow 1 corresponds to v1, etc. (J) Rate equations for each reaction in the model, written using Michaelis Menten kinetics. (K) ODEs representing the rate of change of the concentration of each protein in the model. The rate of change of concentration is equal to the rate of the protein species being made, minus the rate of it being degraded or changed to another state.

Once the qualitative interactions were determined, rate equations were written for each step in the model, assuming Michaelis-Menten kinetics for enzymatic steps, Mass Action kinetics for drug interactions and degradation, and constant rates of synthesis. The initial amount of each element and the values of the parameters were specified. Differential equations were written to describe the rate of change of the concentration of each element. The differential equations are simply equal to the rate of each element being made minus the rate of it changing states, i.e. the rate of the arrows in Figure 3 pointing toward the element minus the ones pointing away from it. The rate equations and differential equations of the model containing apigenin are given in Table 1 and Figure 1, J and K. This first version of

the model was converted into computer code and named “First Model” (See supplementary material 1: Model code).

Validation of the ‘Caspase-3 Regulation Model’

Treatment with chemotherapeutic drugs constitutes one of the most common approaches to eliminate cancer cells (70, 71). Etoposide, a topoisomerase inhibitor, is commonly used to induce cell death. We previously reported that PKCδ-dependent phosphorylation of caspase-3 is necessary in etoposide-induced apoptosis (24). We showed by *in vitro* kinase assays that the activity of PKCδ increased during the first hour of etoposide treatment, reaching a maximum at around 4 h, and then decreased after 8 h (Figure 4, A and (24)). Caspase-3 activity in the same lysates increased starting at around 3 h and continued to increase for the remainder of the time course tested (Figure 4, B and (24)). We used these activation profiles to test whether the model is accurate enough that it fits with previous knowledge of the apoptotic pathway.

To better understand the biological role of PKCδ in caspase-3-dependent apoptosis, we used our mathematical model to represent the biological results. For this purpose, we adjusted the arbitrarily chosen parameters of the “First Model” to find parameter values at which the output from Berkeley Madonna was qualitatively similar to the experimental results (Figure 4, C and (24)). Using this approach we found that PKCδ is inactive at the beginning of the simulation, increases in activity, and then drops back down by hour 5, followed by another increase in activity (Figure 4, C, red line). Caspase-3 was also inactive at the beginning of the simulation, and increased until the simulations stop time (Figure 4, C, blue line). The reason for the oscillations in PKCδ activity and the plateau in caspase-3 activity both beginning at about six and a half hours is unknown but may reflect small

maladjustments in the parameters. Thus, using this model we were able to reproduce the qualitative profile of PKCδ and caspase-3 activation during apoptosis.

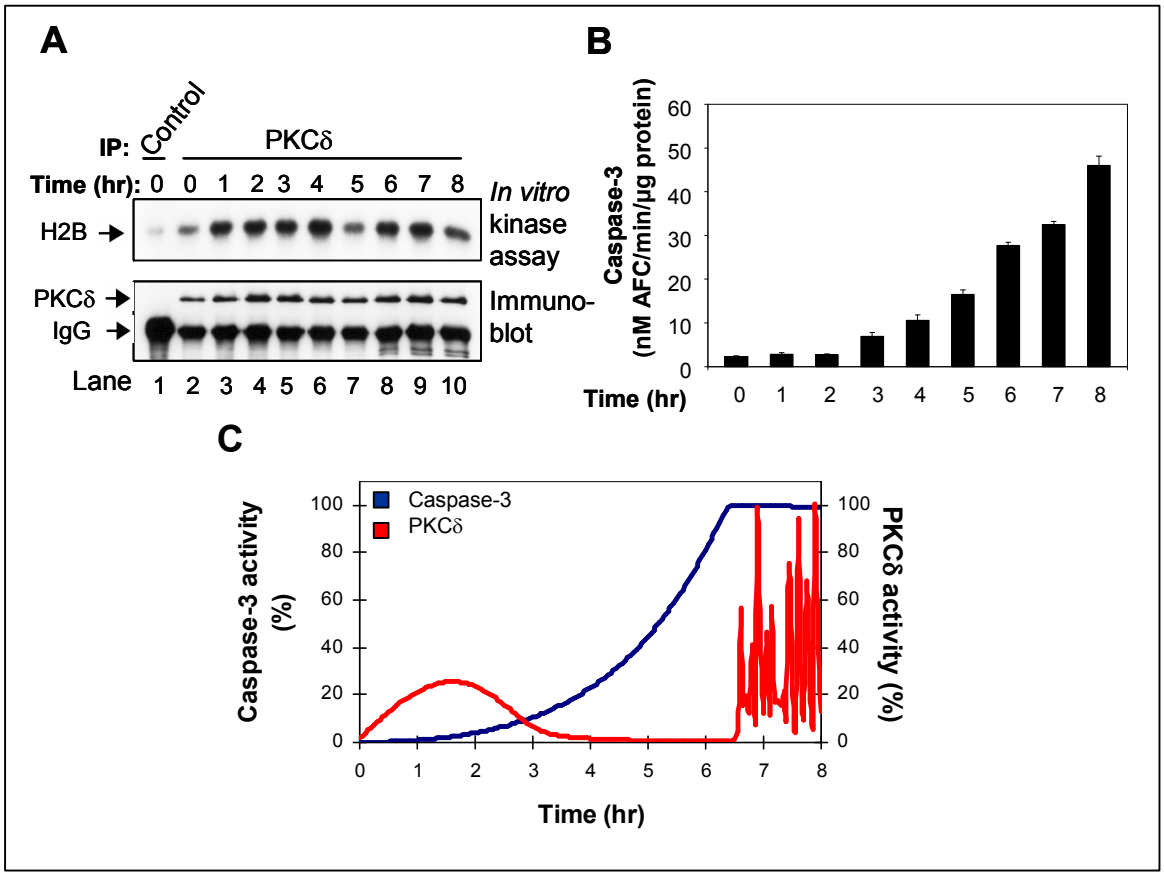

Figure 4 – Model accurately simulates PKCδ and caspase-3 activity in leukemia cells treated with 1 μM etoposide.
(A) Extracts from THP-1 cells cultured for various lengths of time with 1 μM etoposide to induce apoptosis were immunoprecipitated (IP) with anti-PKCδ antibodies and subjected to *in vitro* kinase assay using H2B as substrate in the presence of {γ-^{32}P} ATP. The kinase reaction products were resolved by SDS-PAGE and transferred to a membrane, and phosphorylated H2B was visualized by autoradiography (*upper panel*). The same membrane was immunoblotted with anti-PKCδ antibody to ensure equal loading of the samples *(lower panel)*. The kinase activity shown at the *top* was measured by PhosphorImager and normalized by PKCδ density shown at the *bottom* (24). (B) Caspase-3 activity from the same lysates used in (A) was measured by DEVD-AFC assay (24). (C) Model of the activation of PKCδ (red) and caspase-3 (blue) during etoposide-induced apoptosis. See additional file 1: Model code for the code and additional file 2: Simulation parameters for the parameters used to perform this analysis. The model used is 'First Model' and the set of parameters used in (C) is named 'validation.'

Caspase-3 activation precedes caspase-9 in apigenin-induced-apoptosis

In an attempt to identify novel chemotherapeutic approaches we have identified apigenin, a plant flavonoid as a potent chemotherapeutic agent for leukemia (37). Apigenin

induces apoptosis through the intrinsic pathway mediating the activation of caspase-9 and -3. Since the complex network of the caspase cascade seems to vary depending on the apoptotic stimulus (72), we decided to investigate in more detail the activation of caspase-9 and -3 in apigenin-induced-apoptosis. In light of the fact that the exact mechanism of apigenin has yet to be exposed, we anticipated to gain some insight into this chemotherapeutic drug's line of attack using the mathematical model. Experiments conducted in our laboratory showed that cells treated for different times with apigenin showed increased caspase-9 activity at 6 h and decreasing activity after 12 h of treatment with apigenin (Figure 5, A and (37)). In the same lysates, we found that caspase-3 activity increased at 3 h, remained similar up to 12 h, and decreased after 24 h of apigenin treatment (Figure 5, B and (37)).

In silico experiments based in the kinetics of caspases during etoposide-induced-apoptosis were able to adjust well to the data generated in cells. Due to the successful validation of the model in leukemia cells treated with etoposide, we decided to investigate the caspase cascade during cell death induced by a different drug. The caspase cascade can differ depending on the apoptotic stimulus and apigenin is a good candidate for study since little is known about this relatively new potential chemotherapeutic drug. Hence, we next used this model to study the activation of the caspases during the less characterized system of apigenin-induced-apoptosis. To do this, we simulated the experimental results published by Vargo et al, (Figure 5, A and B) using our *in silico* model (Figure 3). For this purpose we added a term to the rate equation v_3 to account for the effects of apigenin (Figure 3, I and Table 1, *). The new model was named "Api-Model" (See supplementary material 1: Model code). Using this model, we showed that caspase-3 activation quickly reaches high levels, peaking between 9 and 12 hours, before decreasing quickly (Figure 5, B, blue line). This is exactly the same pattern that was seen by Vargo et al (Figure 5, A, (37)). Caspase-9 showed similar behaviour to caspase-3, but peaked sooner, which is also in agreement with

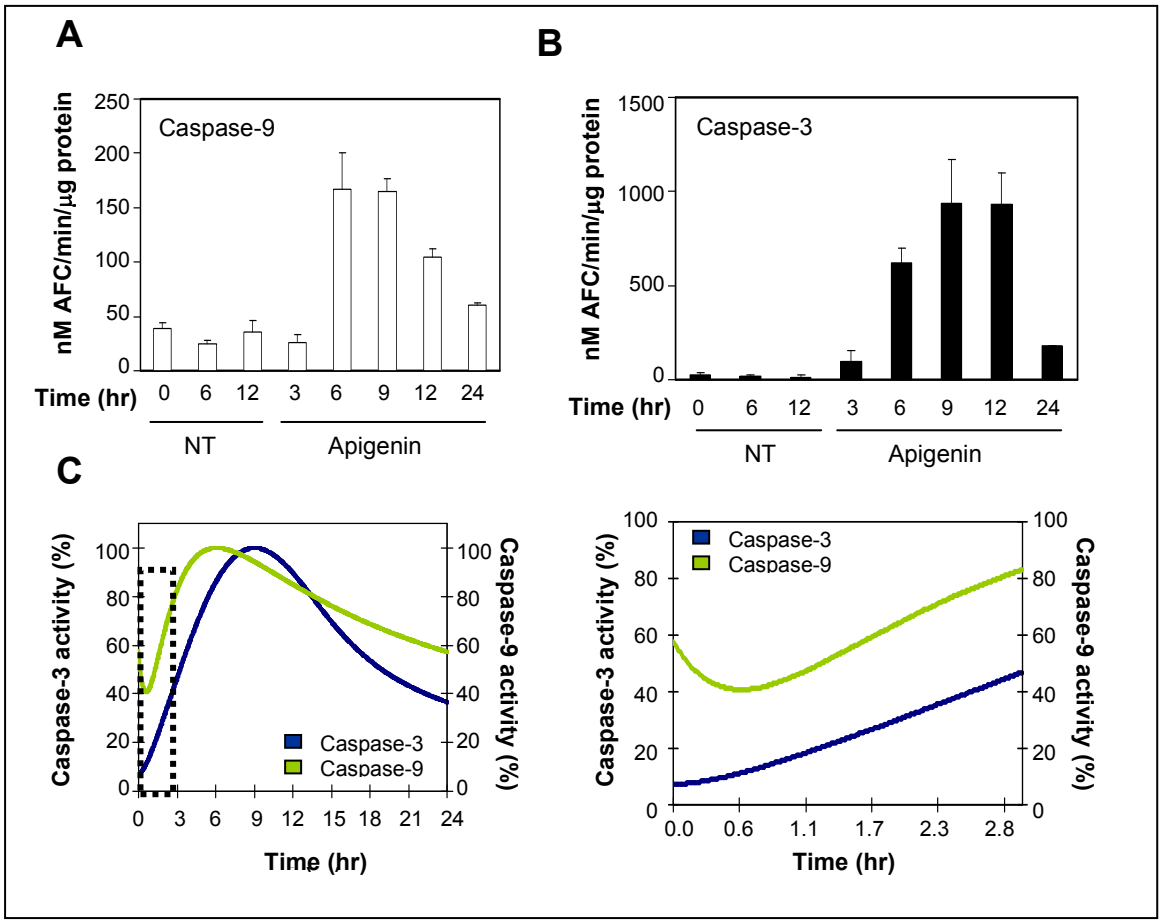

Figure 5 - Model accurately predicts caspase-9 and caspase-3 activity in THP-1 cells in response to treatment with apigenin.
(A) THP-1 cells were treated for various lengths of time with 50 μM apigenin or DMSO (NT) and caspase activity was established. Caspase-9 activity was determined by the LEHD-AFC assay (37). (B) Caspase-3 activity was determined by the DEVD-AFC assay. Data represents means ± S.E.M. (*N* = 3) (37). (C) Model of activation of the activation of caspase-3 (blue) and caspase-9 (green). (D) Enlarged view of the start of caspase activation (Panel 4C) shows that the activity of caspase-3 (blue) begins to increase before caspase-9 activity (green). See additional file 1: Model code for the code and additional file 2: Simulation parameters for the parameters used to perform this analysis. The model used is 'Api-Model' and the set of parameters used is named 'validation 2.'

previously published data (Figure 5, C, green line, A, (37)). In addition, we found that the extent of caspase-9 activity is much lower than caspase-3 activity, as it was in THP-1 cells treated with apigenin (data not shown, Figure 5, A and B, note scales on y axis (37)). Interestingly, a closer look at the earlier times during addition of apigenin indicated that caspase-3 activation preceded the activation of caspase-9 (Figure 5, D). In a classical pathway, caspase-9 is upstream of caspase-3 as part of the intrinsic pathway, so it was expected that caspase-9 activity would increase before caspase-3. These experimental results

suggest the presence of a positive feedback loop between caspase-3 and caspase-9 or one of its upstream elements. A feedback loop in which caspase-3 cleaves caspase-9, resulting in the amplification of both caspases, has previously been identified as necessary for their full activation (14, 17). For caspase-3 to become active before caspase-9, caspase-3 must be able to feedback to activate caspase-9, either directly or indirectly.

Threshold behaviour of caspase-3 in apigenin-induced-apoptosis

Based on our findings that caspase-3 activation occurs prior to caspase-9, we studied the possibility of the existence of thresholds that can regulate the execution of apoptosis. For this purpose, we determined the relationship of caspase-3 activity and its positive regulator PKCδ using our "Caspase-3 Regulation Model." The model was altered slightly to make k_{3a} into a variable rather than a parameter, and named "Threshold model" (See Methods and supplementary material 1: Model code). *In silico* experiments using the "Threshold model" to postulate the effects of PKCδ on caspase activation revealed that k_{3a}, representing the apigenin-dependent rate of activation of PKCδ must reach a threshold in order to activate caspase-3 (Figure 6 and Table 1, at end of text). This simulation also revealed a threshold level of PKCδ activation that must be met before caspase-3 activation occurs, and that caspase-3 protease activity is all-or-none, with no intermediate phase during which caspase-3 is partially active under the conditions of the simulation (Figure 6).

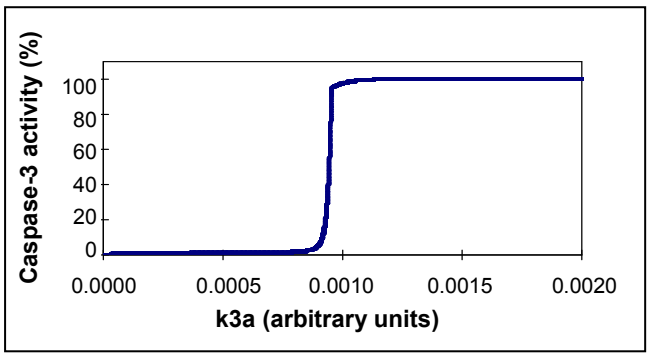

Figure 6 – A threshold of PKCδ is needed for caspases-3 activation.
A threshold of k3a is needed to activate caspases-3. The variable k3a is the apigenin-dependent rate of activation of PKCδ (See Table 1). See additional file 1: Model code for the code and additional file 2: Simulation parameters for the parameters used to perform this analysis. The model used is 'Threshold model' and the set of parameters used is named 'threshold.'

These findings may help explain the inability of certain cancer cells that normally express caspase-9 and -3 to execute cell death (73). The lack of activation of the apoptotic cascade may be due to their lack of the positive action of PKCδ, which may affect the ability of caspase-3 activity to reach an apoptotic threshold. These observations support the use of small molecules that promote PKCδ activity as potential targets to promote apoptosis in cancer cells (74). Drugs that target PKCδ may induce apoptosis in cancer cells by aiding the cell in reaching the threshold needed to activate caspase-3.

Prediction of PKCδ activation profile during apigenin-induced-apoptosis

Apigenin has been shown to induce apoptosis through a mechanism that requires PKCδ activation (37). Since we showed previously that PKCδ positively regulates caspase-3 activation (24), we used the model to simulate the behaviour of PKCδ activity with different concentrations of apigenin. To do this, the model was altered to make apigenin a variable, and named "PKC activity model" (See Methods and supplementary material 1: Model code). According to the model, in the absence of apigenin, PKCδ was inactive, but with even a small amount of apigenin, PKCδ activity increased dramatically, reaching saturation (Figure 7, A). To determine whether the model was able to simulate the biological scenario, we next determined the PKCδ activity in apigenin-treated-cells. For this purpose kinase assays were performed using immunoprecipitates of lysates from cells treated with different doses of apigenin. We found a large increase in PKCδ activity in cells treated with amounts of apigenin as small as 1 μM (Figure 7, B). Increasing concentrations of apigenin induced sustained PKCδ activity and do not activate PKCδ any further. Thus, the experimental data is consistent with the predictions obtained with our model where PKCδ becomes fully active with a very small dose of apigenin, reaching its saturation.

The use of plant polyphenols as neutraceuticals in our diet is gaining momentum as a better understanding of their mechanisms of action becomes recognized (75) (76). Notably, our findings showed that a very small amount of apigenin is necessary to activate PKCδ in cancer cells. Additional experiments to clarify the role of apigenin *in vivo* will further elucidate the possibility of utilizing this compound to the benefit of our health. Our model should facilitate the implementation of biological approaches that will provide a faster assessment in how apigenin, and likely other related flavonoids, regulate cell death.

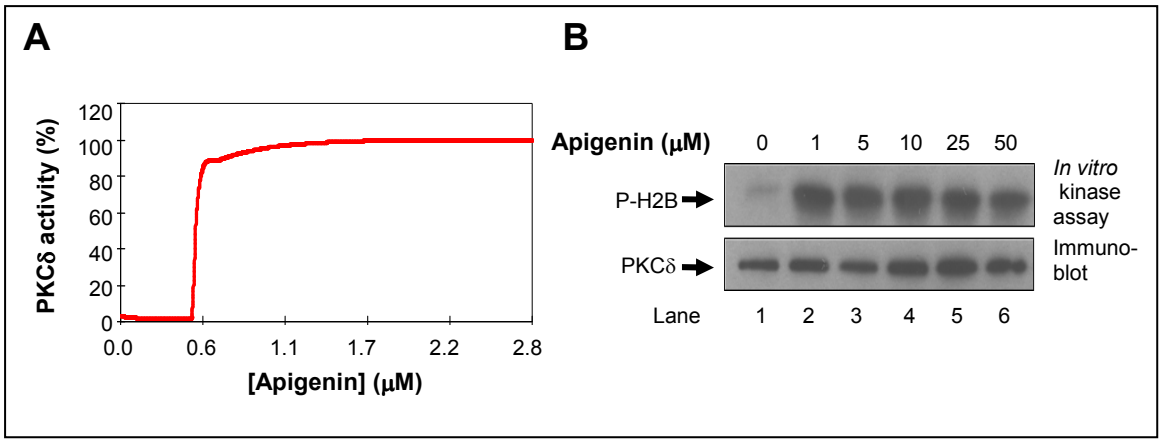

Figure 7 - Experiment confirms model prediction of PKCδ activation by apigenin.
(A) Using the same parameters that validated the model, the activity of PKCδ was simulated at various concentrations of apigenin. See additional file 1: Model code for the code and additional file 2: Simulation parameters for the parameters used to perform this analysis. The model used is 'PKC activity model' and the set of parameters used is named 'PKC prediction.' (B) Lysates from THP-1 cells treated with different concentrations of apigenin were immunoprecipitated with anti-PKCδ antibodies and subjected to *in vitro* kinase assay using H2B as exogenous substrate in the presence of {γ-^{32}P}ATP. The kinase reaction products were analyzed by SDS-PAGE and transferred to a membrane. Autoradiography was used to visualize phosphorylated H2B. The same membrane was immunoblotted with anti-PKCδ antibody to ensure equal loading.

Identification of genes regulated by apigenin

To further elucidate the mechanisms of apigenin-induced-apoptosis, we studied the effects of apigenin in gene expression. There is some evidence that apigenin may modulate transcription, since it has been found to effect several transcription factors known to be involved in apoptosis, including JUN (77), NFκB (41, 78, 79), and c-MYC (80). Therefore, a microarray experiment was conducted to identify genes that exhibit changes in expression

level during apigenin-induced apoptosis. For this purpose, THP-1 leukemia cells were treated either with apigenin or with DMSO, the diluent of apigenin, for 3 h and mRNA was isolated from these samples for hybridization to the microarray. The data was analyzed using the dChip software (50). After normalization, the data was filtered to remove genes with small changes in expression level. Filtering the original 54,676 probe sets resulted in a list of only 1,395 probe sets with large variation across samples that are considered significant. Of these genes, 58% were downregulated, while 42% were upregulated. A selection of the resulting genes with functions relevant to our interests and their fold changes is in Table 3.

To investigate the functions of the genes that had the largest variation in expression, we began by classifying them by their Gene Ontology (GO) terms. The number of genes belonging to each term of the GO Biological Process, Cellular Component, and Molecular Function were counted and graphed in Figure 8. Genes involved in transcription, signal transduction, and protein or nucleic acid binding were among those most frequently found in our data, some being upregulated and others downregulated (Figure 8). This may be indicative of a large-scale shift in the cell, shutting down some pathways and transcriptional programs while turning others on.

One possible mechanism by which apigenin may cause apoptosis is by mediating DNA damage. Our lab has observed histone release from the nucleus into the cytoplasm during apigenin-induced apoptosis, which may be a sign of DNA damage. HIST1H4A (histone cluster 1, H4a), about which very little is known, was seen to be upregulated in our data. NCOA1 (nuclear receptor coactivator 1), a histone acetyltransferase that acts as a cofactor to aid transcription by Jun, NFκB and STAT3, was downregulated and could potential be involved in the observed histone release, although this is only speculation (81). While it is not known if apigenin truly induces DNA damage, if this is the case, it would be expected that DNA repair enzymes would be transcriptionally upregulated in response.

Indeed, it was found that MSH4 (mutS homolog 4), a gene whose protein product is involved in double strand break repair (82), is strongly induced by apigenin, over 11 fold. In addition, two genes TPD52L1 (tumor protein D52-like 1) and CDKN2A (cyclin-dependent kinase inhibitor 2A), which have been suggested to play a role in DNA fragmentation during apoptosis (83, 84) were upregulated by more than 12 fold. We also found that BCL2L11 (BCL2-like 11), a pro-apoptotic member of the BCL2 family that can promote the intrinsic pathway, was downregulated by 6.7 fold (Table 3, at end of text) (85).

Apigenin also has an anti-inflammatory effect, which is not surprising given the links between inflammation, apoptosis, and cancer (32, 1, 86, 87). In addition, JUN and NFκB, two transcription factors known to respond to apigenin, have roles in the immune response (88, 89). Therefore, genes involved in inflammation were also investigated for possible regulation by apigenin. The Toll-Like Receptor (TLR) pathway mediates the immune response by recognizing a variety of pathogens and malignant cells. There are at least 12 TLRs in humans and mice. When bound to a ligand, these receptors activate the NFκB and type I interferon pathways and cause the release of pro-inflammatory cytokines by immune cells (90). It has also been shown that apigenin treatment prevents the release of cytokines in response to LPS (79), which is a ligand for TLR4 (90).

Several genes involved in the TLR pathway were suggested to be downregulated in response to apigenin. The TLR1 receptor is downregulated, as is its downstream effector TRAF6 (TNF receptor-associated factor 6), which is an indirect activator of both JUN and NFκB, and a direct activator the transcription factor IRF5 (interferon regulatory factor 5) (91, 92). JUN and IRF5 themselves are also transcriptionally downregulated. IRF5 and NFκB target several cytokines that are released in response to inflammatory stimulus, including IL-8 (interleukin 8), MIP-1α (chemokine (C-C motif) ligand 3), and MIP-1β (chemokine (C-C motif) ligand 4), which were all downregulated in response to apigenin (93, 94, 95). This is

A

GO Biological Process of upregulated genes after filtering

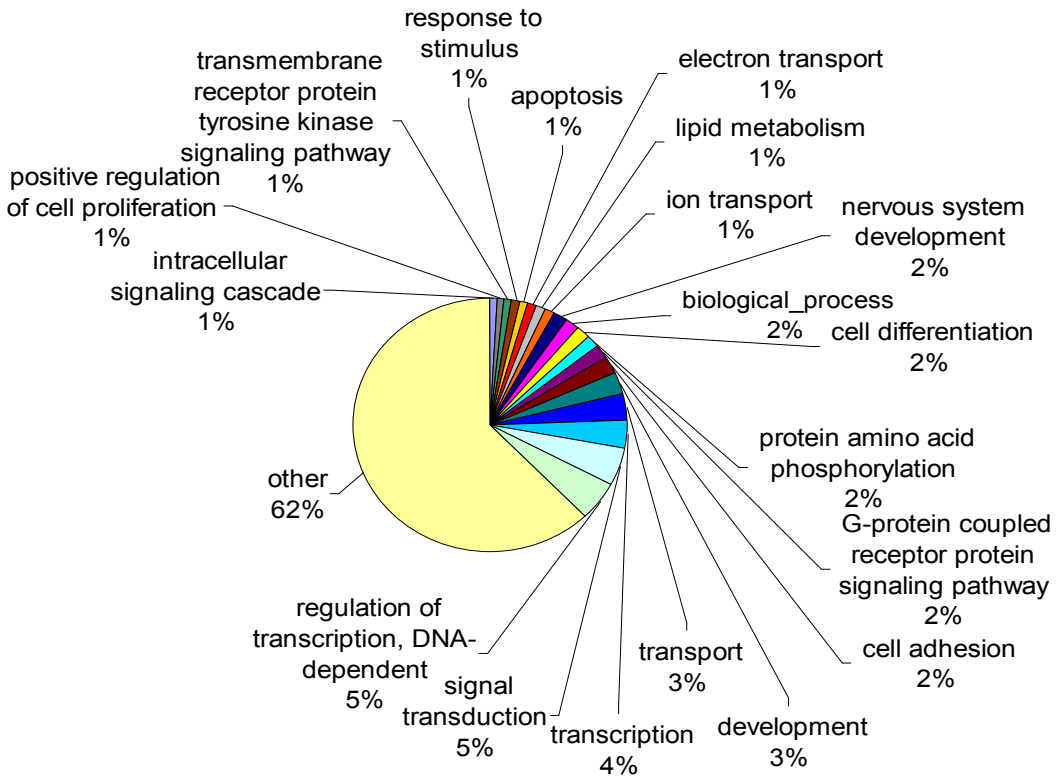

B

GO Biological Process of downregulated genes after filtering

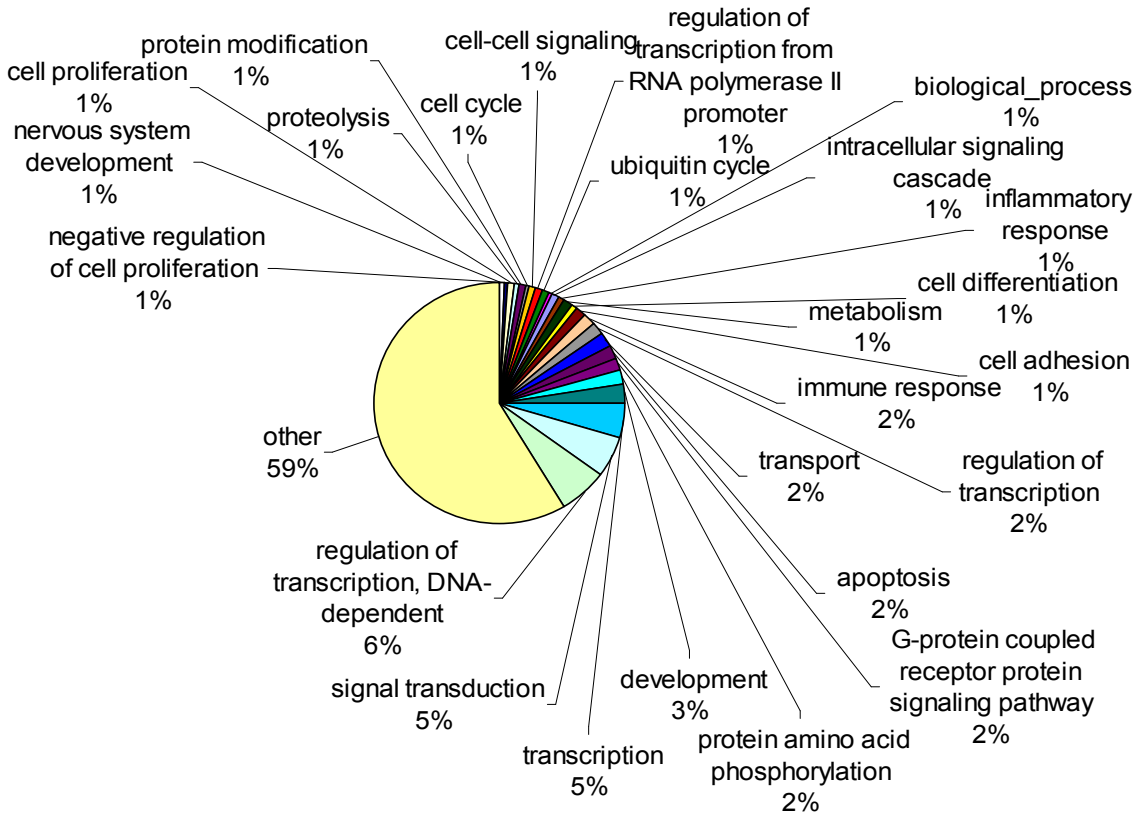

C

GO Cellular Component of upregulated genes after filtering

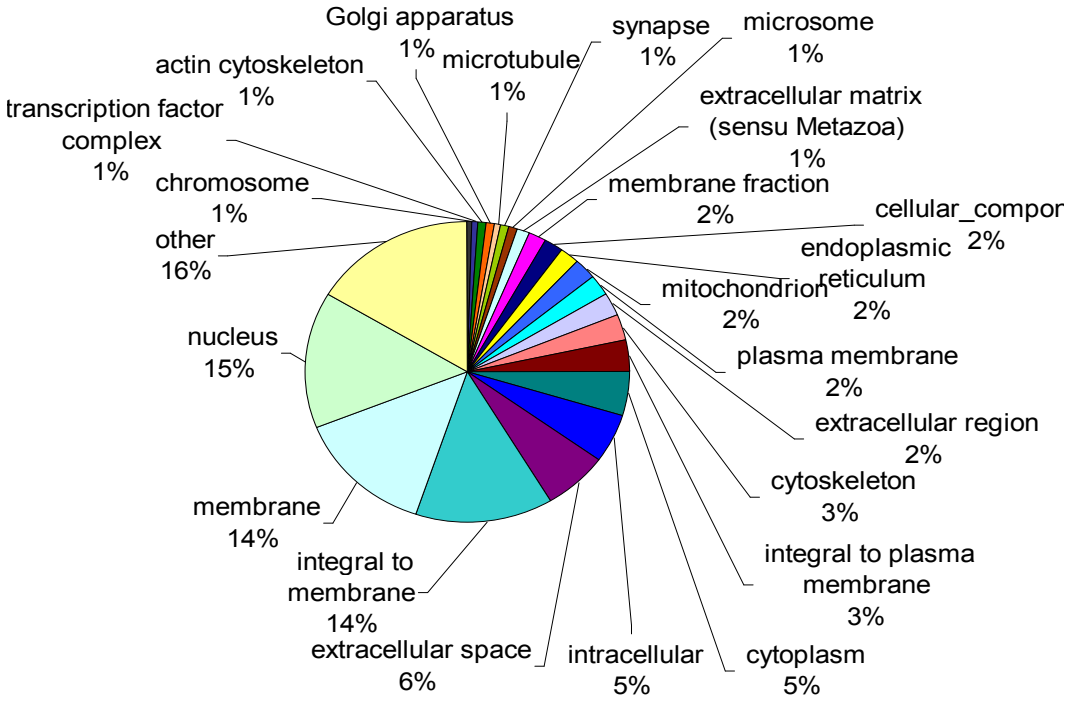

D

GO Cellular Component of downregulated genes afer filtering

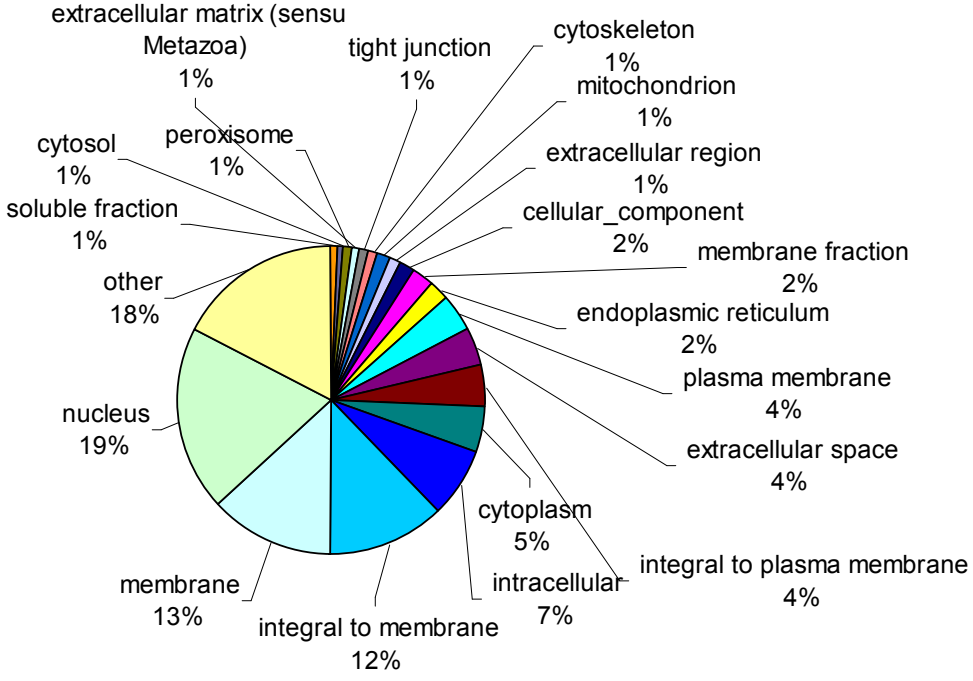

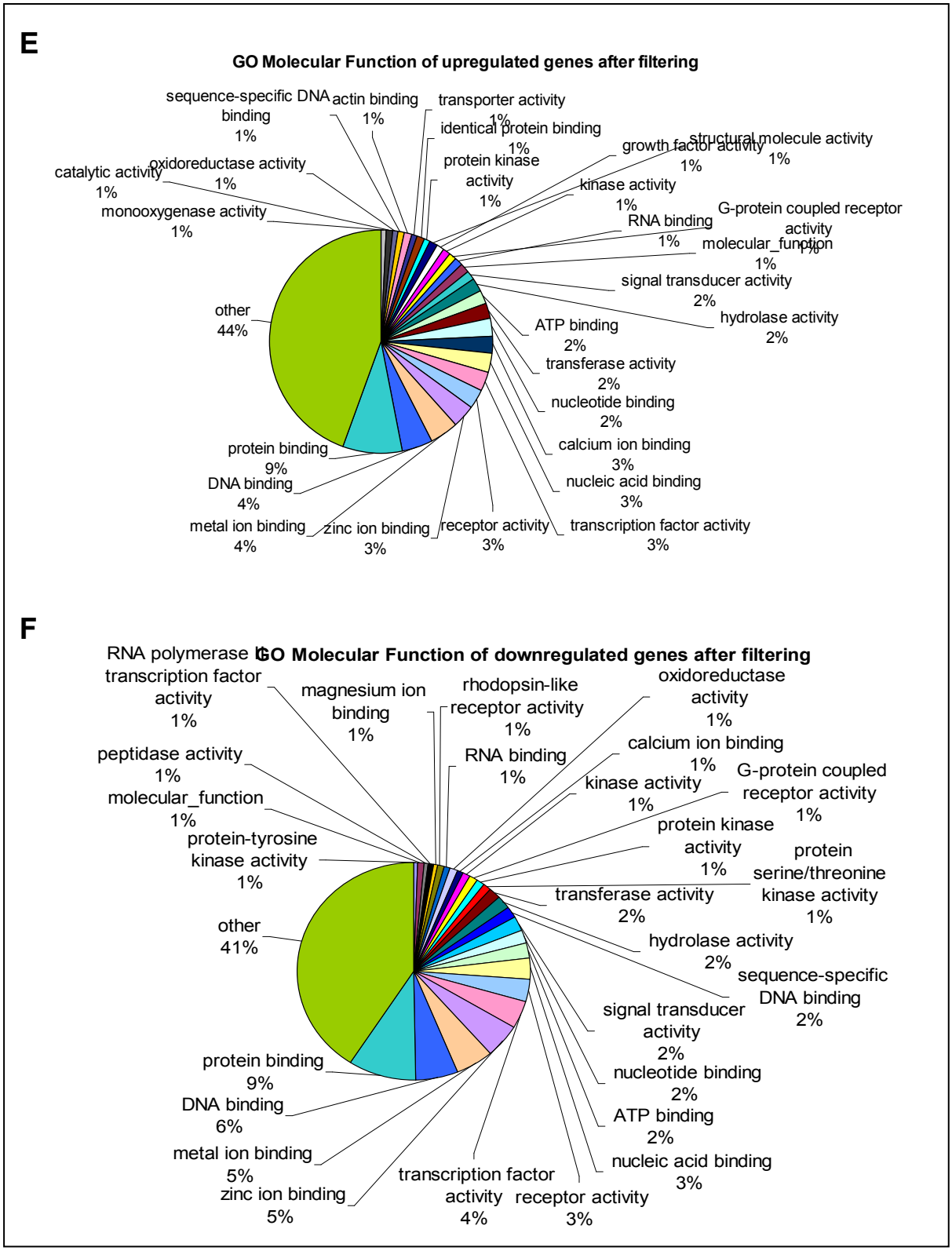

Figure 8- Genes graphed by Gene Ontology.
(A) Percentage of upregulated genes belonging to GO Biological Process terms. (B) Percentage of downregulated genes belonging to GO Biological Process terms. (C) Percentage of upregulated genes belonging to GO Cellular Component terms. (D) Percentage of downregulated genes belonging to GO Cellular Component terms. (E) Percentage of upregulated genes belonging to GO Molecular Function terms. (F) Percentage of downregulated genes belonging to GO Molecular Function terms. Percent of total genes remaining after filtering.

consistent with the finding that IL-8 release in response to LPS is inhibited by apigenin in human monocytes and mouse macrophages (79). COX2 (cytochrome c oxidase II), a target of NFκB which has been shown to be an oncogene and linked to mutagenesis and reduced apoptosis, also shows reduced expression due to apigenin treatment (94, 96) (Table 3, Figure 9). These data may give insight into the mechanism of the anti-inflammatory action of apigenin.

In addition to the DNA repair and TLR pathways, several genes identified by microarray to be regulated by apigenin are directly involved in the apoptotic cascade. FAS and CASP8AP2 (CASP8 associated protein 2), are involved in the extrinsic pathway of apoptosis. FAS is a member of the TNF superfamily of receptors, and acts as a death receptor, recruiting proteins to form the DISC, which activates caspase-8 (97). One of the recruited proteins is CASP8AP2, which is also known as FLASH, and may be necessary for caspase-8 activation (98). Imai et al found that CASP8AP2 has a domain similar in sequence to the ATPase domain of Apaf-1 and may be a functional analogue of Apaf-1 (98). This is disputed however, as Koonin et al were unable to identify any region of similarity between CASP8AP2 and Apaf-1 (99). IRF1 (interferon regulatory factor 1), a transcription factor that induces apoptosis by cleaving caspase-3 in a FADD (and caspase-8 dependent, but death ligand independent, manner was also implicated (101) (Table 3, Figure 10).

Paradoxically, several pro-apoptotic genes were downregulated after apigenin treatment, including FAS, BCL2L11, and caspase-3 (Table 3, Figure 10). This may be partially explained by noting that caspase-3 is a target of IRF5, and FAS is a target of NFκB, transcription factors that may be directly or indirectly downregulated in these conditions (95, 94). Microarrays only measure changes in mRNA expression and it is possible that post-transcriptional and post-translational regulation may increase the activity of these proteins, even if the mRNA encoding them is less abundant.

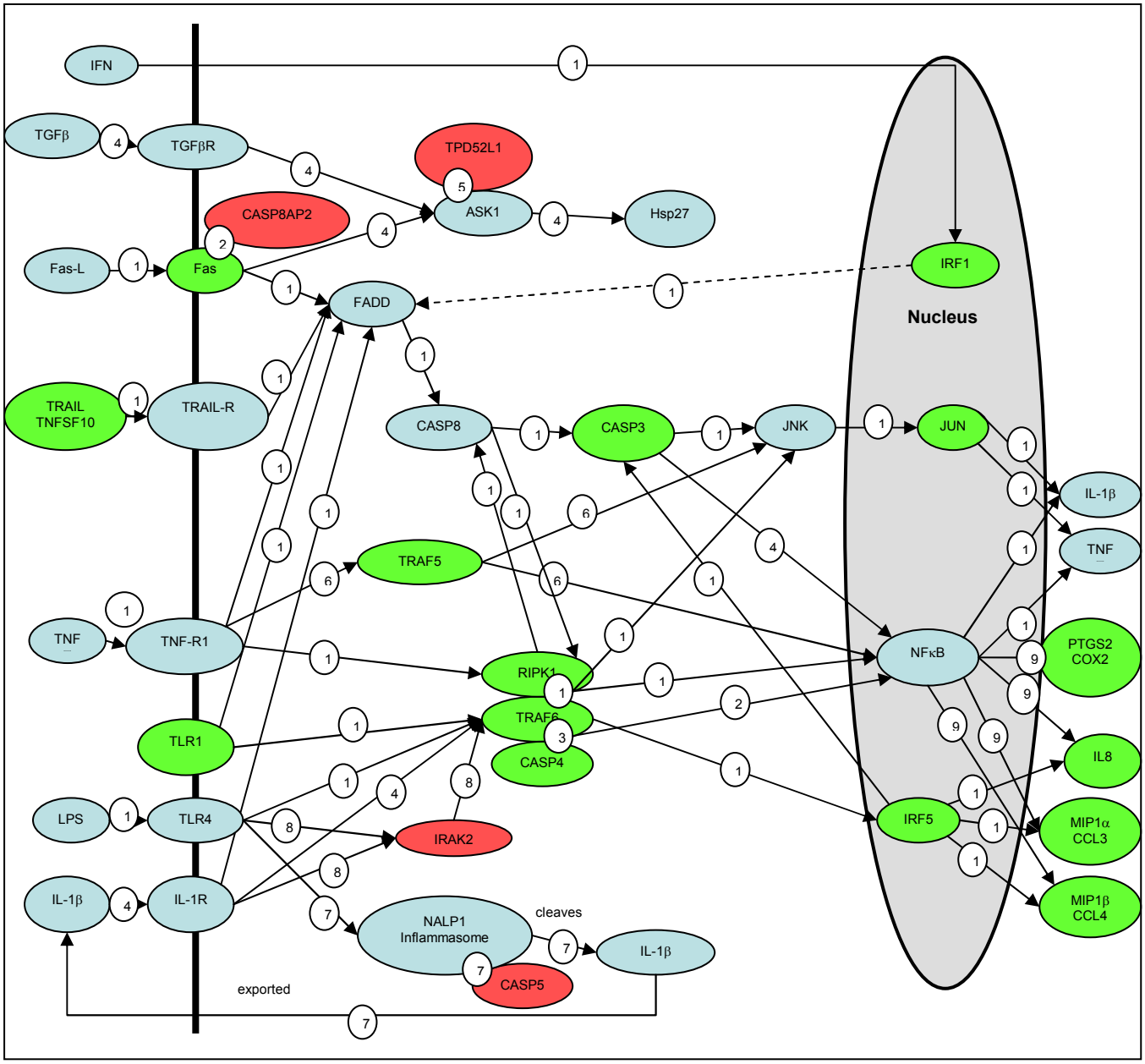

Figure 9- Members of several inflammatory and apoptotic cascades may be transcriptionally regulated in response to apigenin treatment.
Genes from a number of different pathways may be involved in the mechanism of action of apigenin. Blue: no change in expression, Green: downregulation, Red: upregulation. References: 1) (51, 53, 52) 2) (98) 3) (100) 4) (101) 5) (83) 6) (102) 7) (103) 8) (104) 9) (94) 10) (105) 11) (95).

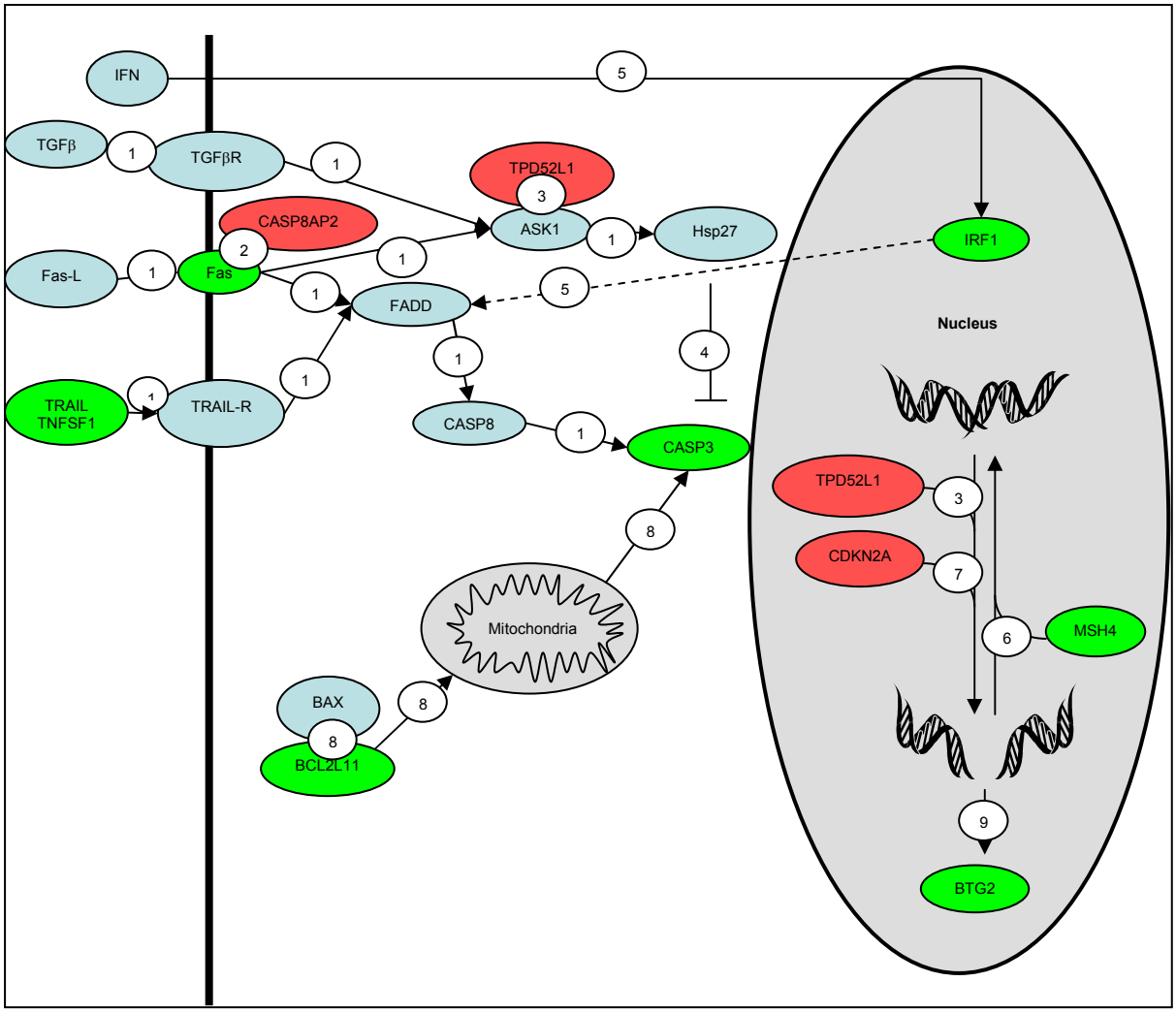

Figure 10- Members of several apoptotic cascades may be transcriptionally regulated in response to apigenin treatment.
Genes from a number of different pathways may be involved in the mechanism of action of apigenin. Blue: no change in expression, Green: downregulation, Red: upregulation. References: 1) (51, 53, 52) 2) (98) 3) (83) 4) (23) 5) (101) 6) (82) 7) (84) 8) (85) 9) (106)

While these genes attract interest due to their known roles in apoptosis, the Toll-like receptor pathway, and DNA repair, the observed changes in their regulation must be confirmed before concrete conclusions can be drawn about their possible involvement in apigenin-induced apoptosis. The genes that have been identified as having particular relevance may be further examined using RT-PCR to confirm changes in expression level under the conditions tested in the microarray, and western blots of the protein products of these genes to tell if changes in expression correlate with changes in protein levels.

Molecular characterization of caspase-3 phosphorylation sites

Since previous knowledge and the "Caspase-3 Regulation Model" both indicate an important role for PKCδ-dependent phosphorylation in the activation of caspase-3 activity, we decided to investigate this means of regulation further. Posttranslational modifications, like phosphorylation and proteolysis, are common methods of modulating protein activity. Posttranslational modifications are known to be especially critical for members of the caspase cascade, many of which are synthesized as inactive precursors to protect the cell against accidental apoptosis (13).

The activity of caspase-3 is regulated by phosphorylation by PKCδ (24). However, to date the location and number of phosphorylation sites that are relevant *in vivo* are unknown. Using *in silico* programs that predict phosphorylation sites, 11 candidate sites were suggested, 8 of which were conserved throughout evolution. Next, mass spectrometry was used to map phosphorylation sites on phosphorylated purified caspase-3. Using this method we found seven sites phosphorylated by PKCδ: Ser12, Ser32, Ser36, Ser58, Thr59, Thr67, and Thr77. *In silico* analysis revealed that all but two, Ser32 and Ser58, of these sites are conserved through evolution. To map the phosphorylation sites and determined their biological function, we began the process of generating phosphomutants of caspase-3. Single sites or combinations of sites were mutated to either alanine, to mimic constitutive non-phosphorylation, or aspartic acid, to mimic constitutive phosphorylation. This broadly used approach has been used to study the phosphorylation of several proteins, including MITF (107), Ets1 and Ets2 (108), TRF1 (109), and CHK2 (110). For a diagram of the experimental scheme, see Figure 11.

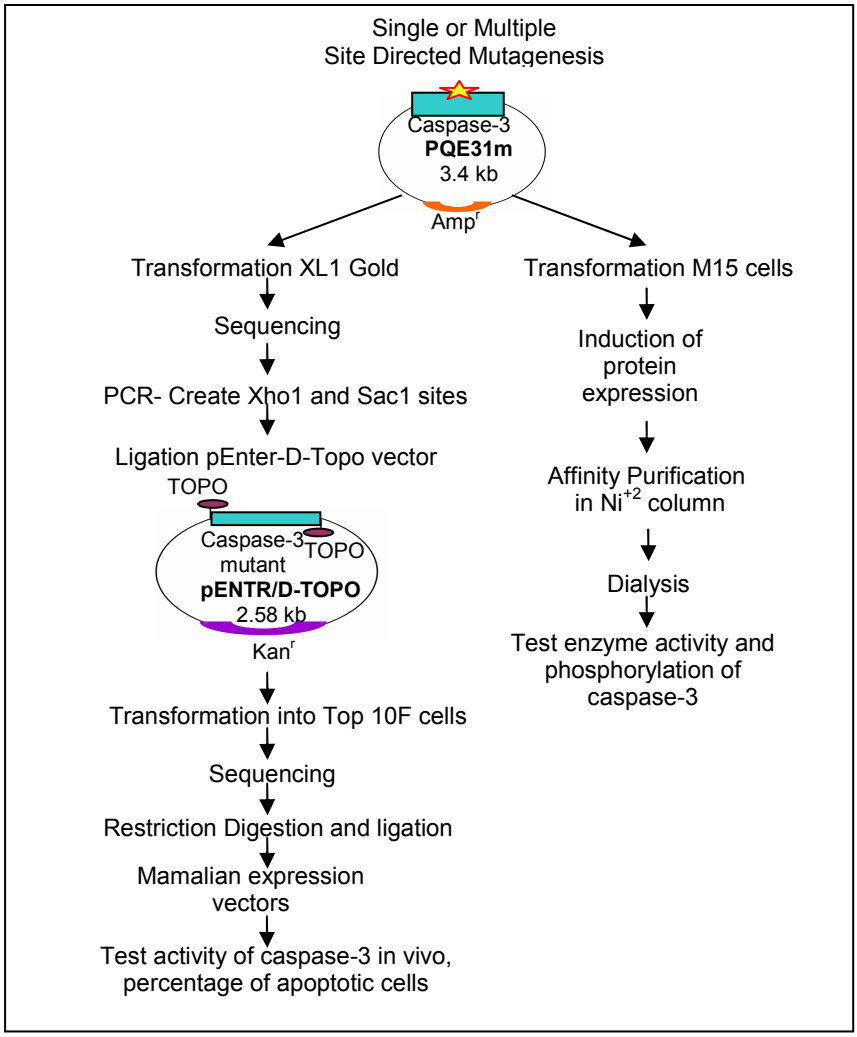

Figure 11- Experimental scheme.
Experiments used to create and examine the activity of caspase-3 mutants in mammalian cells and *in vitro*.

Mutant caspase-3 was created by site directed mutagenesis and introduced into a pQE31 vector in order to add a 6x His tag that would be used later. This insert was then cloned into XL1 Gold and M15 cells. The DNA from the XL1 Gold cells was sequenced to verify that the appropriate mutations were present. PCR was performed to introduce SacI and XhoI sites and the PCR product was ligated into p-ENTR/D-TOPO. This vector was used for the ease and efficiency of ligating a small insert with only one small sticky end using the topoisomerase linked to the vector. The vector was transformed into Top10F cells and sequenced again to ensure no unwanted mutations had been introduced. The plasmid was also digested using SacI and XhoI to check for the presence of insert (Figure 12, A). This insert was finally cloned into pDs-red or pCMV, which are mammalian expression vectors.

The mutant activity of the caspase-3 proteins will be investigated by determining the percent apoptotic cells when treated with an apoptotic stimulus, and comparing to the wild type.

The DNA that was cloned into M15 cells was used for *in vitro* analysis. Expression of mutant caspase-3 was induced using IPTG and caspase-3-mutant protein was purified from bacteria using a Ni^{2+}-NTA affinity column (see Material and Methods). Using a discontinuous imidazol gradient, we obtained caspase-3 protein at elutions corresponding to 100 mM imidazol as determined by SDS-PAGE (Figure 12, B, lanes 20 and 21).

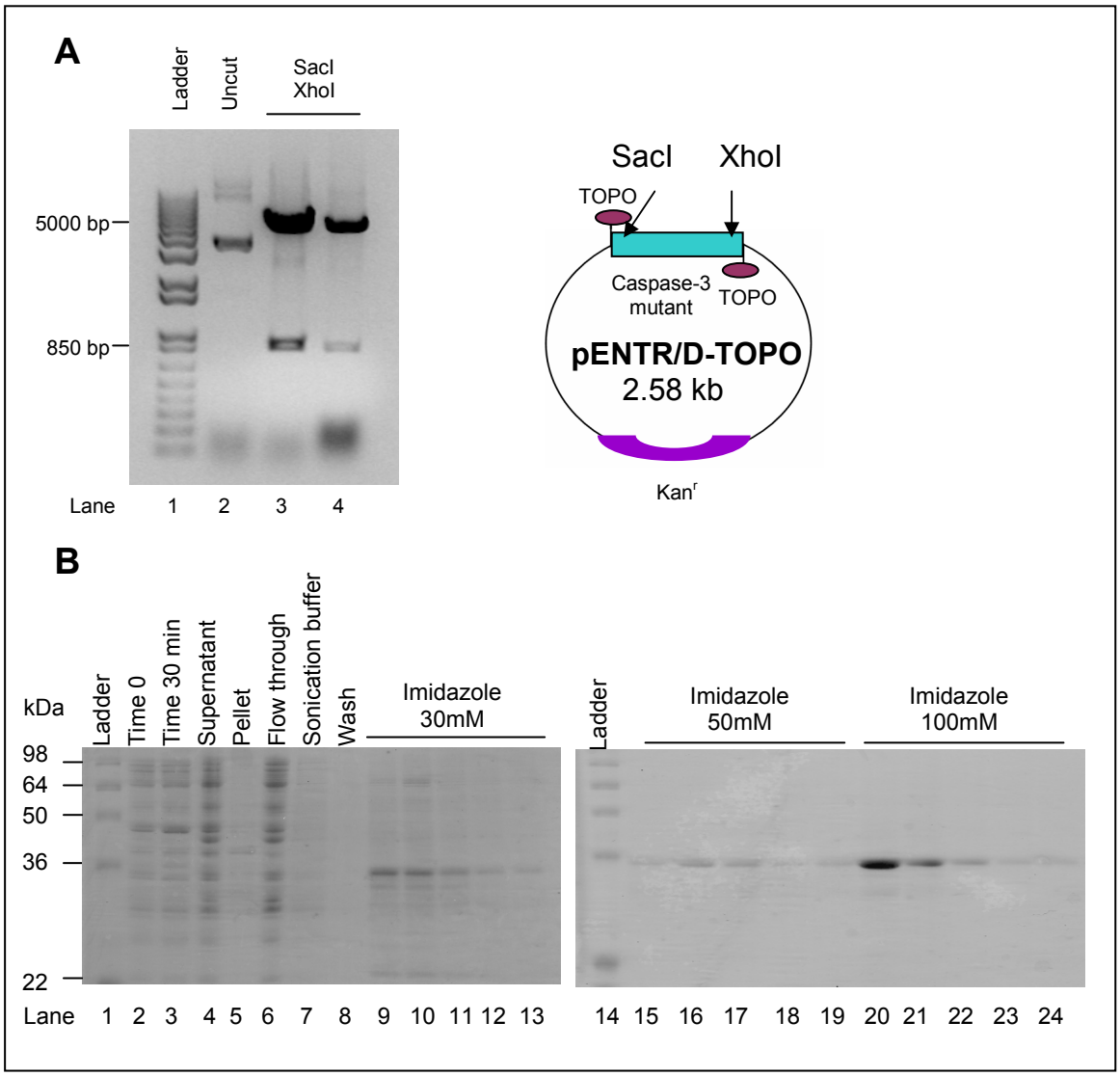

Figure 12- Cloning and protein purification.
(A) Representative gel of caspase-3 insert digested from a d-TOPO vector using SacI and XhoI (caspase-3 wt full length, 850 bp) (B) Purification of Asp77 using a Ni2+-NTA affinity column with elutions in a discontinuous gradient of imidazole. Elution fractions containing mutant caspase-3 were identified by SDS-PAGE.

After dialysis, the activity of the mutant caspase-3 was investigated using a caspase-3 activity assay. Caspase-3 was activated by incubation with caspase-9, promoting the first cleavage of caspase-3, at 37°C for various time points, up to 2 h. After activation, a known specific substrate of caspase-3, a DEVD peptide, conjugated to the fluorescent molecule AFC, was added to the active enzyme. Caspase-3 cleavage frees AFC, allowing it to fluoresce. The amount of fluorescence was measured to determine the activity of caspase-3. It is expected that mutants containing aspartic acid at a phosphorylation site will show faster activation, since this negatively charged amino acid mimics phosphorylation, and phosphorylation has been shown to increase caspase-3 activity (24).

Much more work must be done to definitively map the PKCδ phosphorylation sites of caspase-3. More mutants will be created, and the activities of each mutant protein will be tested to determine which sites are important for caspase-3 activity *in vitro*. *In vitro* kinase assays will be performed on the alanine mutants, to determine which sites are phosphorylated. Since alanine cannot be phosphorylated, a mutant with an important site changed to alanine should show less PKCδ-dependent phosphorylation than the wild type. Furthermore, to enable an application to human health, the relevance of these sites to caspase-3 activation *in vivo* must also be determined. This work entails the creation and analysis of many mutants and is as yet uncompleted.

Structural characterization of caspase-3 phosphorylation sites

In order to narrow down the list of which sites may be phosphorylated by PKCδ *in vivo*, structural analysis was performed on six of these sites, in parallel with the molecular studies. This approach has been extensively used to make predications about protein functions and mechanisms based on structural information. An impediment in our study was the lack of available crystal structure for full-length caspase-3. We based our prediction on

the structure of an enzyme composed of the p17 and p12 domains of caspase-3, and lacking the amino-terminal pro domain, which has never been crystallized because it is too disordered (111). We are aware of the limitations that this implies but rationalize that structural predictions could help to focus our work and help to explain some of our results. Ser12 is in the pro domain of caspase-3, and therefore cannot be studied by this approach. The remaining six sites are found in the p17 domain. The crystal structure of caspase-3, with the locations of the sites of interest, is shown in Figure 13.

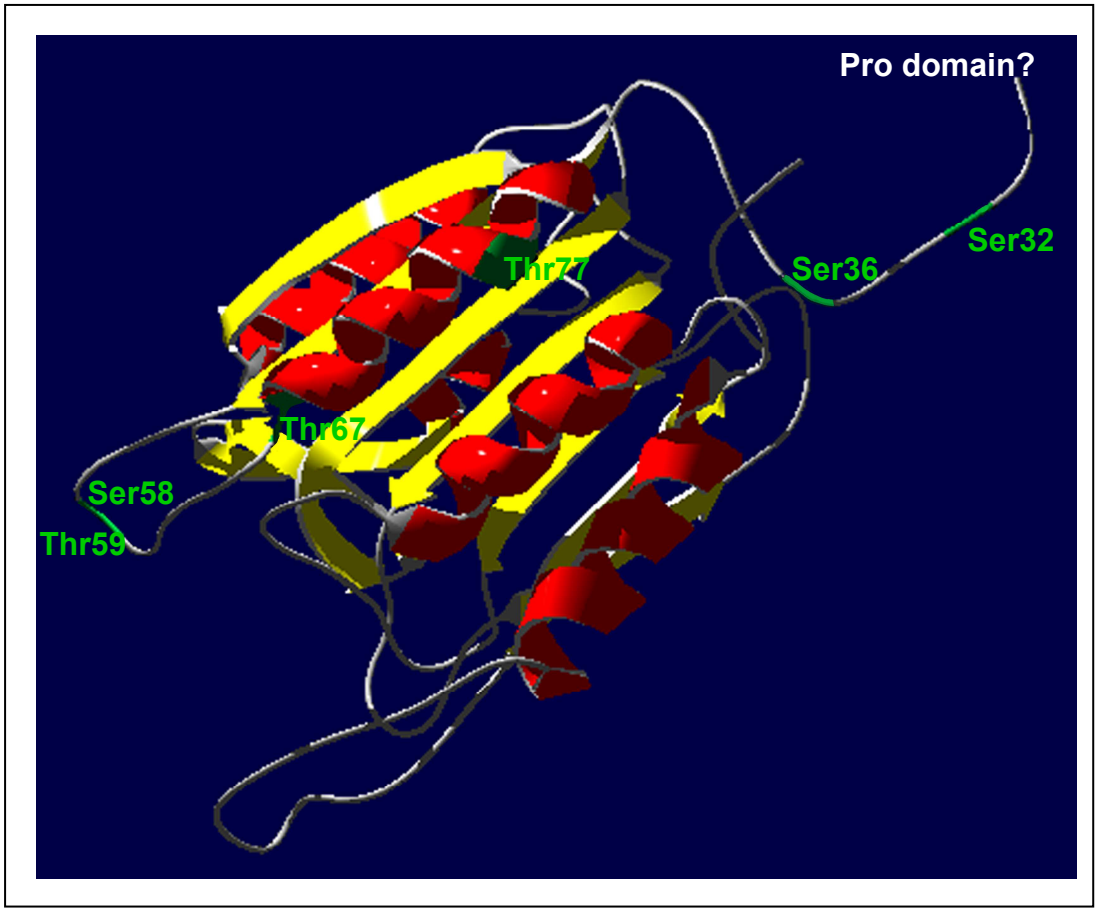

Figure 13- Structure of caspase-3.
Structure of the p17 and p12 domains of caspase-3 with the sites under investigation highlighted. The missing pro domain would be at the N-terminus, with an unknown structure and position. Red: alpha helix, yellow: beta sheet, gray: loops, green: sites of interest.

Since apoptosis is an evolutionarily conserved mechanism, amino acids that are essential to the regulation of caspase-3 are expected to be conserved. We examined the

amino acid alignment of predicted structures of caspase-3 from animals (Figure 14). Alignments that take structure into account may differ from sequence alignments because sequence alignments allow gaps that are not present in the structure of the protein. The serines at positions 32 and 58 are not conserved in the same location in other mammals, and so these sites cannot be phosphorylated by the serine/threonine kinase PKCδ in every mammal. Ser36, Thr59, Thr67, and Thr77 were conserved across mammals, making them more likely candidates for phosphorylation by PKCδ. These four sites were conserved even further down the phylogenetic tree: Ser36 was also conserved in chicken, Thr59 was conserved in chicken, zebrafish, and frog, Thr67 was conserved in chicken and fruit fly, and Thr77 was conserved in fruit fly (Figure 14). This same approach was also used to compare the structural alignment of the effector caspases -3, -6, and -7, which have similar sequences and functions. Thr59 and Thr67 were conserved in caspase-7, but none of the sites were conserved in caspase-6 (Figure 15).

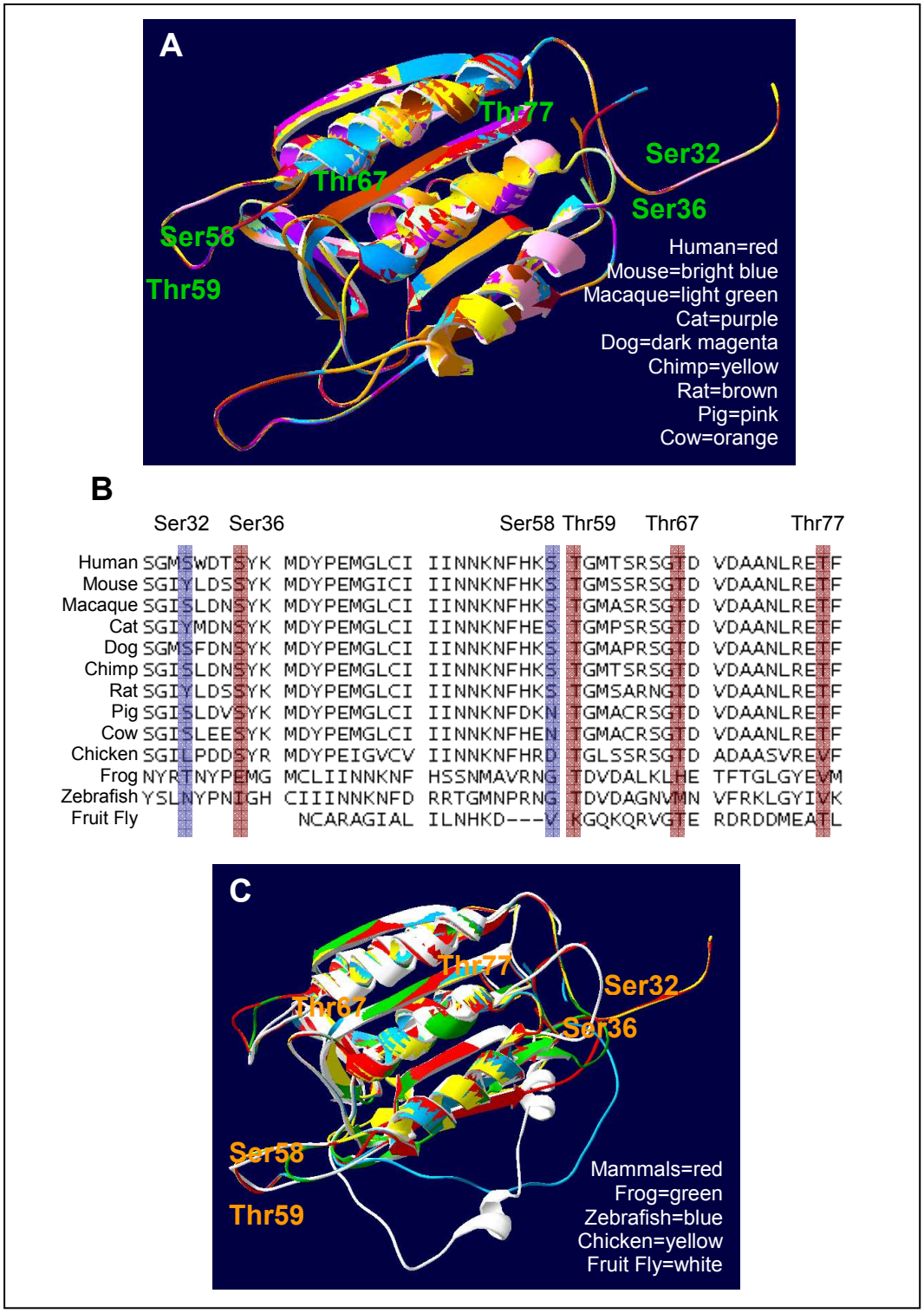

Figure 14- Evolutionary conservation of phosphorylation sites.
(A) Superimposed images of caspase-3 from mammals. (B) Alignment of caspase-3 of various animals from amino acids corresponding to 29 to 78 in human. This alignment takes structure into account, and shows which amino acids are superimposed in (A). red: conserved in mammals, blue: not conserved in mammals.
(C) Superimposed images of mammalian homologues of caspase-3 with homologues from frog, zebrafish, chicken, and fruit fly.

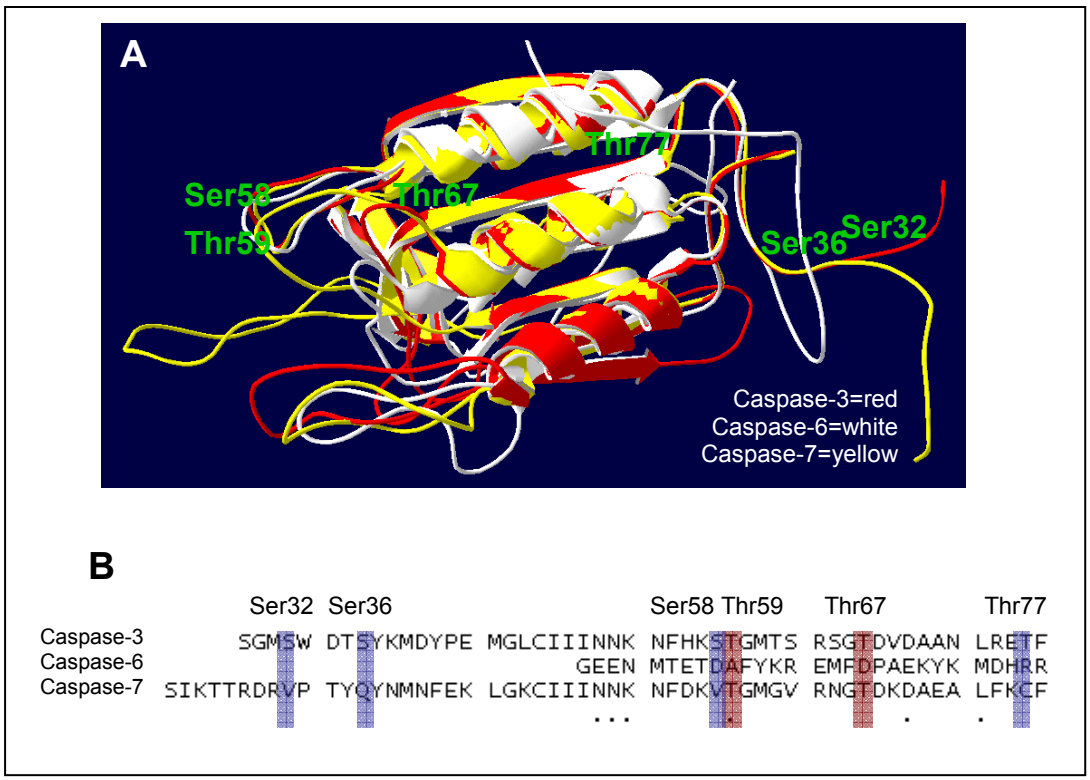

Figure 15- Evolutionary conservation of phosphorylation sites in effector caspases.
(A) Superimposed images of human caspase-3, caspase-6, and caspase-7. (B) Alignment of effector caspases from amino acids corresponding to 29 to 78 in caspase-3. This alignment takes structure into account, and shows which amino acids are superimposed in (A). red: conserved between caspase-3 and caspase-7, blue: not conserved.

It is also important to determine whether or not these sites are accessible to a kinase. The accessibility of these six sites, as well as Thr130 and Ser150 was addressed. Thr130 aligns with Thr125 of caspase-9, which is phosphorylated by ERK in mammalian cell extracts, inhibiting caspase-9 activity (112). Caspase-3 however has not been described as a target of ERK. Ser150 of caspase-3 is known to be phosphorylated by p38, resulting in decreased activity and stability of caspase-3 (113). Caspase-3 is activated by two sequential cleavages, the first of which cuts between the p17 and p12 domains. Therefore, we also considered the accessibility of the sites on a structure containing only the p17 domain (Figure 16, Table 4). Ser36 and Thr77 became much more accessible with the removal of the p12 domain. The accessibilities are shown in Table 4. Ser150, which is known to be phosphorylated by another kinase, has a lower accessibility than all of the sites except for

Thr77 when both domains are considered and Thr67 in both cases (Table 4). These data suggest that many of our sites are highly accessible to a kinase and that Ser36, in particular, may be an important phosphorylation site, since it is both conserved and highly accessible.

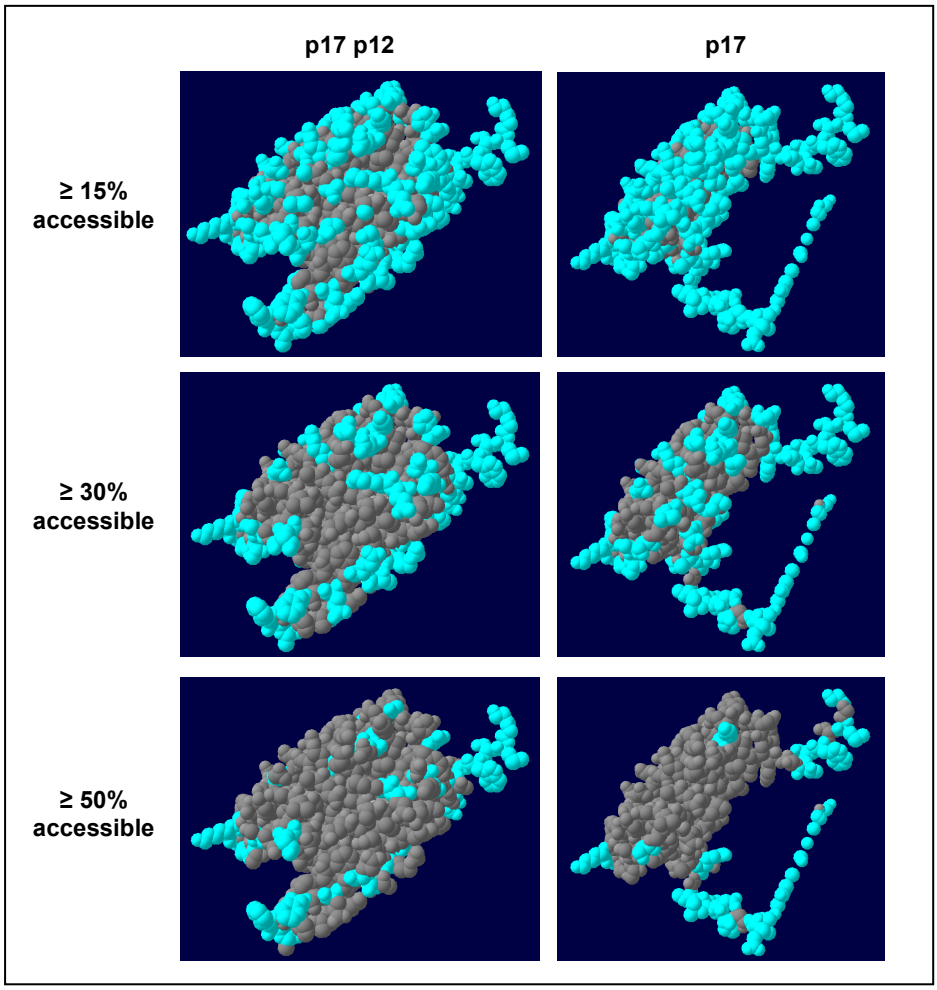

Figure 16- Surface accessibility of amino acids in caspase-3.
Percent of amino acid surface area that is exposed to the exterior. A space filling view of the side chains is shown. Blue: accessibility at or above percent given, gray: accessibility below percent given.

Table 4 – Percent surface accessibility of amino acids of interest

Accessibility	p17 p12	p17
< 5%	Thr67 Thr77 Thr130	Thr67 Thr130
10% - 15%	Ser150	Ser150
20% - 25%	Ser36 Thr59	Thr59

25% - 30%		Thr77
45% - 50%		Ser32 Ser36
50% - 55%	Ser32	
55% - 60%	Ser58	Ser58

Surface accessibility of the six potential PKCδ phosphorylation sites and two additional sites, Thr130 and Ser150, on the p17 and p12 domains of caspase-3 and on the p17 domain alone. Amino acids with increases in accessibility after removal of the p12 domain are highlighted in blue.

Discussion and conclusions

The complex mechanisms by which caspase-3 activity is regulated have been investigated using a multidisciplinary approach. We have built a model of the intrinsic pathway of apoptosis that includes the impact of PKCδ and caspase-3 during apoptosis induced by chemotherapeutic agents. Based on these predictions, we determined the biological behaviour of PKCδ, a positive regulator of apoptosis, *in vivo*. These findings showed that we were able to validate our model of apigenin-induced-apoptosis in a biological system. Using this model, we made predictions about how apigenin, a poorly characterized plant compound, induces apoptosis. This model can be expanded for further explorations, providing a more rapid approach to assess the potential of new drugs in the regulation of apoptosis.

Interestingly, the model predicted that caspase-3 could become activated before caspase-9 during apigenin-induced-apoptosis. This is curious, since it is widely believed that caspase-9 activity is required to activate caspase-3 in the intrinsic pathway, and caspase-8 activation was not observed in apigenin treated cells (37). Therefore, it is not clear how caspase-3 activation begins in these cells. In this regard, the presence of the "safety catch" regulatory peptide, which keeps the caspase-3 proenzyme inactive, could serve as a regulatory region that under certain circumstances could explain the activation of caspase-3 in the absence of caspase-9 activity (114). Caspase-3 has also been shown to be activated by other caspases, including caspase-11 (115). The oligomerization model also suggests that caspase-3 could become active without the aid of any other caspase, if it is present at high enough concentrations to bring two molecules close enough for intermolecular autocatalysis (10)

This latter model is complicated by the fact that caspase-3 was shown to be transcriptionally downregulated by about 8 fold in response to apigenin. This observation

must be treated with caution because it has not been confirmed by other experiments and may be a false result. Even if true, it is possible that changes in transcription levels do not correlate with protein levels in this case. It has been found in yeast that genes showing even a 30 fold change in transcription can maintain a steady state at the protein level (116). Indeed, it has been shown that caspase-3 protein levels remain constant throughout apoptosis (117, 11). It seems that caspase-3 is regulated primarily at the post-transcriptional level, rather than the transcriptional level.

One post-transcriptional modification, the phosphorylation of caspase-3 by PKCδ, is also being investigated by a variety of approaches, although the work has not been completed. *In silico* investigation of the protein structure has led to insights into which potential PKCδ-dependent phosphorylation sites should be the focus of our first efforts at molecular characterization. Mutagenesis, cloning, protein purification, and assays to measure mutant caspase-3 activity are underway. Phosphorylation by PKCδ is a novel mechanism and understanding this level of caspase-3 regulation will greatly add to the basic knowledge of apoptosis. This understanding will translate into improved treatments for the multitude of human diseases that have been linked to deregulated apoptosis.

Acknowledgements

Thanks to Dr. Andrea Doseff for her guidance and support. Thanks to Dr. Baltazar Aguda, Yadira Malavez, Oliver Voss, Melissa Vargo, and Amit Sharma for their contributions to the work, and to the entire Doseff lab for their willing help and advice. Cell culture and caspase activity assays for the mathematical model were performed by Ms. Vargo. Immunoprecipitation and *in vitro* kinase assay was performed by Dr. Doseff. Treatment of cells and RNA isolation for the microarray was performed by Amit Sharma. The research was supported by funding from the National Science Foundation-MCB-0542244 and National Institutes of Health RO1HL075040 to AID and the OSU College of Biological Sciences Dean's Undergraduate Research Fund and Mayers Summer Research Internship to JMD.

Tables

Table 1 - ODE's and rate equations describing mathematical model.

Rate Equation	Explanation
$v_1 = \frac{k_{1a} \times C3_a \times C9}{K_{m1a} + C9} + \frac{k_{1b} \times C9}{K_{m1b} + C9}$	First term: D, Second term: A
$v_2 = \frac{k_{2a} \times C9_a \times C3}{K_{m2a} + C3} + \frac{k_{2b} \times C3_a \times C3}{K_{m2b} + C3} + \frac{k_{2c} \times PKC\delta_a \times C3}{K_{m2c} + C3}$	First term: B, Second term: C, Third term: G
$*v_3 = k_{3a} \times PKC\delta \times Api + k_{3b} \times PKC\delta$	First term: I, absent in model without apigenin, Second term: other means of activation
$v_4 = k_4$	Synthesis
$v_{-4} = \frac{k_{-4a} \times C3_a \times IAP}{K_{m-4a} + IAP} + k_{-4b} \times IAP$	First term: F, Second term: other means of degradation
$v_{-5} = \frac{k_{-5a} \times IAP \times C3_a}{K_{m-5a} + C3_a} + k_{-5b} \times C3_a$	First term: E, Second term: other means of degradation
$v_{-6} = k_{-6} \times C9_a + \frac{k_{-6b} \times IAP \times C9_a}{K_{m-6b} + C9_a}$	First term: other means of degradation, Second term: E
$v_{-7} = k_{-7} \times C9$	Degradation
$v_8 = k_8$	Synthesis
$v_{-8} = k_{-8} \times C3$	Degradation
Ordinary differential equations	**Explanation**
$\frac{d(C9)}{dt} = v_7 - (v_{-7} + v_1)$	Synthesis-(Degradation+Activation)
$\frac{d(C9_a)}{dt} = v_1 - v_{-6}$	Activation-Degradation
$\frac{d(C3)}{dt} = v_8 - (v_{-8} + v_2)$	Synthesis-(Degradation+Activation)
$\frac{d(C3_a)}{dt} = v_2 - v_{-5}$	Activation-Degradation
$\frac{d(IAP)}{dt} = v_4 - v_{-4}$	Synthesis-Degradation
$\frac{d(PKC\delta_a)}{dt} = v_3 - v_{-3}$	Activation-Relocalization
$\frac{d(PKC\delta)}{dt} = v_{-3} - v_3$	Inactive-Activation

Subscript numbers refer to numbers near the arrows in Figure 1. Letters in Explanation column refer to letters in Fig. 1. C3 and C9 stand for casapse-3 and caspase-9, respectively. Subscript "a" denotes active protein. PKCδ stands for both inactive PKCδ and relocalized PKCδ. *For the version of the model that lacks apigenin, $v_3 = k_{3b} \times PKC\delta$.

Table 2 – Literature values for rate constants

Parameter	Rate Constant	Reference
k_{1a}	3.57 x 10^{-3} s^{-1}	(118) (converted to s^{-1})
K_{m1a}	5.56 nM	(118) (converted to s^{-1})
k_{1b}	---	
K_{m1b}	---	
k_{2a}	1.01 min^{-1}	(118)
K_{m2a}	1.39 x 10^{-7} M	(119)
k_{2b}	3.57 x 10^{-3} s^{-1}	(118) (assumed same as $k_{1a,}$ converted to s^{-1})
K_{m2b}	5.56 nM	(118) (assumed same as $K_{m1a,}$ converted to s^{-1})
k_{2c}	---	
K_{m2c}	---	
k_{3a}	---	
k_{3b}	---	
k_{-3a}	3.57 x 10^{-3} s^{-1}	(118) (assumed same as $k_{1a,}$ converted to s^{-1})
K_{m-3a}	5.56 nM	(118) (assumed same as $K_{m1a,}$ converted to s^{-1})
k_{-3b}	8.02 x 10^{-6} s^{-1}	(120) (converted to s^{-1})
k_4	0.04 nM s^{-1}	(49)
k_{-4a}	3.57 x 10^{-3} s^{-1}	(118) (assumed same as $k_{1a,}$ converted to s^{-1})
K_{m-4a}	5.56 nM	(118) (assumed same as $K_{m1a,}$ converted to s^{-1})
k_{-4b}	6 x 10^{-3} s^{-1}	(121)
k_{-5a}	1 x 10^{-3}	(49)
K_{m-5a}	---	
k_{-5b}	1 x 10^{-3} s^{-1}	(49)
k_{-6a}	1 x 10^{-3} s^{-1}	(49)
k_{-6b}	1 x 10^{-3}	(49)
K_{m-6b}	---	
k_7	0.02 nM s^{-1}	(49)
k_{-7}	1 x 10^{-3} s^{-1}	(49)
k_8	0.2 nM s^{-1}	(49)
k_{-8}	3.5 x 10^{-5} s^{-1}	(122) (calculated from half life)
Api	0-50 μM	Used in experiments

Literature values of rate constants with references.

Table 3 – Microarray results of interest

Gene	Probe Set	Fold Change	About	References
HIST1H4A	208046_at	7.33407		
FAS (CD95)	215719_x_at	0.100296	TNF family of receptors. Induces apoptosis.	(97)
	216252_x_at	0.152671		
CASP8AP 2 (FLASH)	1570001_at	35.94334	Structure of Cajal bodies. May be needed to activate caspase-8. Inhibits signalling of glucocorticoid receptor.	(123, 98, 124)
CASP4	213596_at	0.143098	Inflammatory caspase. Interacts with TRAF6. Leads to NFκB activation and cytokine secretion.	(100)
IRF6	1552478_a_at	15.47631	Transcription factor. Van der Woude Syndrome (developmental disorder characterized by cleft lip/palate).	(125)
BCL2L11 (BIM)	1555372_at	0.149572	Downregulated in prostate cancer. Expression is inhibited by NFκB.	(41, 126)
JUN (AP1)	201466_s_at	0.105048	Transcription factor. Phosphorylated by JNK. Required for progression thru G1. Regulated by growth factors, cytokines, oxidative stress, and UV. Proliferative and anti-apoptotic functions. Apigenin decreases levels of JUN.	(88, 77)
IRF1	202531_at	0.170219	Transcription factor. Induces apoptosis. Required for the action of several chemotherapeutic drugs.	(101)
TNFSF10 (TRAIL)	202688_at	0.107112	Required for apoptosis in inactive CD8+ cells.	(127)
	202687_s_at	0.138739		
IRF5	205468_s_at	0.162689	Type I interferon and TLR pathways. Systemic lupus erythematosus, rheumatoid arthritis, inflammatory bowel disease, and MS. Innate immunity. Required for DNA damage induced apoptosis and tumor suppression.	(128, 129)
TRAF5	204352_at	0.103122	CD40 signalling. NFκB activation. B and T cell signalling, organogenesis, cell survival. Mediates NFκB, MAPK, and JNK pathways.	(130, 102)
TRAF4	202871_at	0.161888	Expressed in undifferentiated cells. Low TRAF4 expression correlates to more invasive breast cancer.	(91, 131)
TPD52L1 (D53)	203786_s_at	15.12698	None detected in children diagnosed with ALL or AML. Upregulated during G2/M transition MAPKKK that activates JNK and p38 cascades. Calcium signalling.	(132, 133, 83)
CASP3	236729_at	0.124807	Effector caspase. Activated by the initiator caspases, including caspase-8 and caspase-9. Protease.	(10, 11, 16).
CASP5	207500_at	11.17689	Inflammatory caspase. Activated by the NALP1 inflammasome. Causes cytokine release through NFκB. Apoptosis.	(103, 134)
IRAK2	1553739_at	10.93345	Activation of NFκB. IL-1R and TLR4 signalling. May be involved in	(104, 135)

			carcinogenesis.	
PTGS2 (COX2)	204748_at	0.154179	Linked to mutagenesis, mitogenesis, angiogenesis, reduced apoptosis, metastasis, and immunosuppression	(96)
IL8	202859_x_at	0.139883	Target of IRF5. Target of NFκB. Apigenin treated monocytes and mouse macrophages have reduced production of IL8.	(51, 52, 53, 79, 94)
TRAF6	205558_at	0.069604	IL1 and IL18 signalling. Activates JNK and NFκB. Interacts with IRAK.	(91)
TLR1	210176_at	0.152558	Response to invading pathogens. MyD88-dependent signalling for release of cytokines.	(136, 90)
	239021_at	0.154856		
RIPK1 (RIP1)	226551_at	0.054569	Needed for casp8 activation. Apoptosis. Activation of NFκB and JNK. Serine/threonine kinase.	(105)
CCL3 (MIP-1α)	205114_s_at	0.070623	Target of IRF5. Ligand of CCR1 and CCR5 receptors. Chemokine. Induced by LPS, IL-1β, IFN-γ.	(51, 52, 53, 137, 138)
CCL4 (MIP-1β)	234616_at	0.133971	Target of IRF5. Chemokine. Induced by LPS or IL-7.	(51, 52, 53, 138)
MSH4	210533_at	11.18889	Meitotic and mitotic DNA double strand break repair and DNA damage response. Required for meiosis. Complexes with MSH5. ATP catalysis. Resolving Holliday junctions. No shown role in mismatch repair	(82)
HMOX1	203665_at	0.028441	Converts heme into bile pigments. Source of carbon monoxide, which is involved in inflammation, proliferation, apoptosis. Induced by stress, ROS, LPS, IL-1α IL-1β, IL-6, IL-11, TNFα.	(139)
BTG2	201235_s_at	0.118314	Tumor suppressor. Induced by p53-dependent mechanism and may be involved in cell cycle control and response to DNA damage. Directly or indirectly regulates transcription of cyclin D1.	(140, 106, 141)
ESCO2	241252_at	0.037344	Acetyltransferase. Required for sister chromatid cohesion during S phase. Roberts Syndrome (craniofacial defects, loss of cohesion at centromere and Y chromosome).	(142)

Selected genes with a significant fold change.

Supplementary materials

Supplementary material 1 – Model code

```
{First Model}
```

```
METHOD RK4
STARTTIME = 0
STOPTIME = 100
DT = 0.01

{differential equations}

d/dt(C9) = v7-(vm7+v1)
d/dt(C9a) = v1-vm6
d/dt(C3) = v8-(vm8+v2)
d/dt(C3a) = v2-vm5
d/dt(IAP) = v4-vm4
d/dt(PKCa) = v3-vm3
d/dt(PKCi) = vm3-v3

v1 = k1a*C3a*C9/(KKm1a+C9) + k1b*C9/(KKm1b+C9)
v2 = k2a*C9a*C3/(KKm2a+C3)
       + k2b*C3a*C3/(KKm2b+C3)
       + k2c*PKCa*C3/(KKm2c+C3)
v3 = k3b*PKCi
vm3 = km3a*C3a*PKCa/(KKm3a+PKCa) + km3b*PKCa
v4 = k4
vm4 = km4a*C3a*IAP/(KKm4a+IAP)+km4b*IAP
vm5 = km5a*IAP*C3a/(KKm5a+C3a)+km5b*C3a
vm6 = km6a*C9a + km6b*IAP*C9a/(KKm6b+C9a)
v7 = k7
vm7 = km7*C9
v8 = k8
vm8 = km8*C3

init C9 = 0
init C9a = 0.001
init C3 = 1.0
init C3a = 0.001
init IAP = 0.1
init PKCa = 0.01
init PKCi = 0.07

k1a = 0.1
KKm1a =0.01
k1b = 0.1
KKm1b = 0.001
k2a = 0.4
KKm2a=0.01
k2b = 0.4
KKm2b=0.01
k2c = 0.4
KKm2c=0.01
k3b = 0.2
km3a = 10
KKm3a =0.01
km3b = 1.0
k4 = 0.5
km4a = 0.1
KKm4a = 0.01
km4b = 1.5
km5a = 0.16
KKm5a=0.01
km5b= 0.16
km6a = 0.3
km6b = 1
```

```
KKm6b = 0.001
k7 = 0.5
km7 = 0.1
k8 = 0.08
km8 = 0.08
{End}


{Api-Model}

METHOD RK4
STARTTIME = 0
STOPTIME = 100
DT = 0.01

{differential equations}

d/dt(C9) = v7-(vm7+v1)
d/dt(C9a) = v1-vm6
d/dt(C3) = v8-(vm8+v2)
d/dt(C3a) = v2-vm5
d/dt(IAP) = v4-vm4
d/dt(PKCa) = v3-vm3
d/dt(PKCi) = vm3-v3

v1 = k1a*C3a*C9/(KKm1a+C9) + k1b*C9/(KKm1b+C9)
v2 = k2a*C9a*C3/(KKm2a+C3)
       + k2b*C3a*C3/(KKm2b+C3)
       + k2c*PKCa*C3/(KKm2c+C3)
v3 = k3a*PKCi*Api+(k3b*PKCi)
vm3 = km3a*C3a*PKCa/(KKm3a+PKCa) + km3b*PKCa
v4 = k4
vm4 = km4a*C3a*IAP/(KKm4a+IAP)+km4b*IAP
vm5 = km5a*IAP*C3a/(KKm5a+C3a)+km5b*C3a
vm6 = km6a*C9a + km6b*IAP*C9a/(KKm6b+C9a)
v7 = k7
vm7 = km7*C9
v8 = k8
vm8 = km8*C3

init C9 = 0
init C9a = 0.001
init C3 = 1.0
init C3a = 0.001
init IAP = 0.1
init PKCa = 0.01
init PKCi = 0.07

k1a = 0.1
KKm1a =0.01
k1b = 0.14
KKm1b = 0.001
k2a = 2
KKm2a=0.001
k2b = 0.34
KKm2b=0.001
k2c = 5
KKm2c=0.001
k3a = 0.8
k3b = 0.2
km3a = 10
```

```
KKm3a =0.01
km3b = 1.0
k4 = 0.39
km4a = 0.1
KKm4a = 0.01
km4b = 0.7
km5a = 1.57
KKm5a=0.001
km5b= 5
km6a = 0.3
km6b = 1
KKm6b = 0.001
k7 = 0.16
km7 = 0.05
k8 = 0.08
km8 = 0.08
Api = 50
{End}


{Threshold model}

METHOD RK4
STARTTIME = 0
STOPTIME = 100
DT = 0.01

{differential equations}

d/dt(C9) = v7-(vm7+v1)
d/dt(C9a) = v1-vm6
d/dt(C3) = v8-(vm8+v2)
d/dt(C3a) = v2-vm5
d/dt(IAP) = v4-vm4
d/dt(PKCa) = v3-vm3
d/dt(PKCi) = vm3-v3
d/dt(k3a) = 0.00001

v1 = k1a*C3a*C9/(KKm1a+C9) + k1b*C9/(KKm1b+C9)
v2 = k2a*C9a*C3/(KKm2a+C3)
       + k2b*C3a*C3/(KKm2b+C3)
       + k2c*PKCa*C3/(KKm2c+C3)
v3 = k3a*PKCi*Api+k3b*PKCi
vm3 = km3a*C3a*PKCa/(KKm3a+PKCa) + km3b*PKCa
v4 = k4
vm4 = km4a*C3a*IAP/(KKm4a+IAP)+km4b*IAP
vm5 = km5a*IAP*C3a/(KKm5a+C3a)+km5b*C3a
vm6 = km6a*C9a + km6b*IAP*C9a/(KKm6b+C9a)
v7 = k7
vm7 = km7*C9
v8 = k8
vm8 = km8*C3

init C9 = 0
init C9a = 0.001
init C3 = 1.0
init C3a = 0.001
init IAP = 0.1
init PKCa = 0.01
init PKCi = 0.07
init k3a = 0
```

```
k1a = 1.0
KKm1a =0.01
k1b = 0.1
KKm1b = 0.001
k2a = 0.4
KKm2a=0.01
k2b = 0.4
KKm2b=0.01
k2c = 0.4
KKm2c=0.01
k3b = 0.2
km3a = 10
KKm3a =0.01
km3b = 1.0
k4 = 0.5
km4a = 0.1
KKm4a = 0.01
km4b = 1.5
km5a = 0.16
KKm5a=0.01
km5b= 0.16
km6a = 0.3
km6b = 1
KKm6b = 0.001
k7 = 0.5
km7 = 0.1
k8 = 0.08
km8 = 0.08
Api = 50
{End}


{PKC activity model}

METHOD RK4
STARTTIME = 0
STOPTIME = 100
DT = 0.01

{differential equations}

d/dt(C9) = v7-(vm7+v1)
d/dt(C9a) = v1-vm6
d/dt(C3) = v8-(vm8+v2)
d/dt(C3a) = v2-vm5
d/dt(IAP) = v4-vm4
d/dt(PKCa) = v3-vm3
d/dt(PKCi) = vm3-v3
d/dt(Api) = 0.00001

v1 = k1a*C3a*C9/(KKm1a+C9) + k1b*C9/(KKm1b+C9)
v2 = k2a*C9a*C3/(KKm2a+C3)
       + k2b*C3a*C3/(KKm2b+C3)
       + k2c*PKCa*C3/(KKm2c+C3)
v3 = k3a*PKCi*Api+(k3b*PKCi)
vm3 = km3a*C3a*PKCa/(KKm3a+PKCa) + km3b*PKCa
v4 = k4
vm4 = km4a*C3a*IAP/(KKm4a+IAP)+km4b*IAP
vm5 = km5a*IAP*C3a/(KKm5a+C3a)+km5b*C3a
vm6 = km6a*C9a + km6b*IAP*C9a/(KKm6b+C9a)
```

```
v7 = k7
vm7 = km7*C9
v8 = k8
vm8 = km8*C3

init C9 = 0
init C9a = 0.001
init C3 = 1.0
init C3a = 0.001
init IAP = 0.1
init PKCa = 0.01
init PKCi = 0.07
init Api = 0

k1a = 0.1
KKm1a=0.01
k1b = 0.14
KKm1b = 0.001
k2a = 2
KKm2a=0.001
k2b = 0.34
KKm2b=0.001
k2c = 5
KKm2c=0.001
k3a = 0.8
k3b = 0.2
km3a = 10
KKm3a=0.01
km3b = 1.0
k4 = 0.39
km4a = 0.1
KKm4a = 0.01
km4b = 0.7
km5a = 1.57
KKm5a=0.001
km5b= 5
km6a = 0.3
km6b = 1
KKm6b = 0.001
k7 = 0.16
km7 = 0.05
k8 = 0.08
km8 = 0.08
{End}
```

Code for the models used in Berkeley Madonna.

Supplementary material 2 – Simulation parameters

parameter	First Model	validation	oscillation	Api-Model	validation 2
stoptime	100	1.6	40	100	0.16
k1a	0.1	0.1	0.07	0.1	0.1
KKm1a	0.01	0.01	0.01	0.01	0.01
k1b	0.1	0.1	0.05	0.14	0.1
KKm1b	0.001	0.001	0.001	0.001	0.0042
k2a	0.4	3.17	0.01	2	1

KKm2a	0.01	0.01	0.01	0.001	0.001
k2b	0.4	2.44	0.75	0.34	0.68
KKm2b	0.01	0.01	0.01	0.001	0.001
k2c	0.4	0.3	1	5	7.1
KKm2c	0.01	0.01	0.01	0.001	0.001
k3a	N/A	N/A	N/A	0.8	0.8
k3b	0.2	1	0.38	0.2	0.2
km3a	10	3.7	0.92	10	10
KKm3a	0.01	0.01	0.01	0.01	0.01
km3b	1	0.1	0.001	1	1
k4	0.5	0.07	0.5	0.39	1
km4a	0.1	0.1	0.01	0.1	0.01
KKm4a	0.01	0.01	0.01	0.01	0.01
km4b	1.5	0.1	1.5	0.7	0.01
km5a	0.16	0.01	0.16	1.57	4.1
KKm5a	0.01	0.01	0.01	0.001	0.001
km5b	0.16	0.01	0.15	5	10
km6a	0.3	0.01	0.92	0.3	2
km6b	1	0.01	0.001	1	2.1
KKm6b	0.001	0.001	0.001	0.001	0.001
k7	0.5	0.5	0.5	0.16	0.4
km7	0.1	0.1	0.1	0.05	0.001
k8	0.08	0.001	0.08	0.08	0.08
km8	0.08	0.01	0.08	0.08	0.08
Api	N/A	N/A	N/A	50	50
init PKCa	0.01	0.001	0.001	0.01	0.01
init C9a	0.001	0.001	0.001	0.001	2.00E-04
init C3a	0.001	0.001	0.001	0.001	2.00E-04

Supplementary material 2- Simulation parameters - Continued

parameter	Threshold model	threshold	PKC activity model	pkc prediction
stoptime	100	200	100	25
k1a	1	1	0.1	0.1
KKm1a	0.01	0.01	0.01	0.01
k1b	0.1	0.02	0.14	0.28
KKm1b	0.001	0.001	0.001	0.001
k2a	0.4	0.45	2	2.335
KKm2a	0.01	0.01	0.001	0.001
k2b	0.4	0.4	0.34	0.399
KKm2b	0.01	0.01	0.001	0.001
k2c	0.4	0.02	5	1.38
KKm2c	0.01	0.01	0.001	0.001
k3a	N/A	N/A	0.8	0.8
k3b	0.2	0.2	0.2	0.091
km3a	10	10	10	10
KKm3a	0.01	0.01	0.01	0.01
km3b	1	1	1	1
k4	0.5	0.5	0.39	0.39

km4a	0.1	0.1	0.1	0.1
KKm4a	0.01	0.01	0.01	0.01
km4b	1.5	1.5	0.7	0.7
km5a	0.16	0.16	1.57	1.57
KKm5a	0.01	0.01	0.001	0.001
km5b	0.16	0.16	5	5
km6a	0.3	0.3	0.3	0.3
km6b	1	0.04	1	0.23
KKm6b	0.001	0.001	0.001	0.001
k7	0.5	0.5	0.16	0.16
km7	0.1	0.1	0.05	0.05
k8	0.08	0.16	0.08	0.08
km8	0.08	0.175	0.08	0.08
Api	50	50	N/A	N/A
init PKCa	0.01	0.01	0.01	0.01
init C9a	0.001	0.001	0.001	0.001
init C3a	0.001	0.001	0.001	0.001

The parameters used for each validation and simulation.

Supplementary material 3 – Dimensionless equations

Dimensionless Equations

$$\frac{1}{k_{-7}}\frac{d\xi_9}{dt} = h_7 - h_1\frac{\xi_{3a1}\xi_9}{1+\xi_9} - h_{1b}\frac{\xi_9}{p_{m1}+\xi_9} - \xi_9$$

$$\frac{1}{k_{-6}}\frac{d\xi_{9a}}{dt} = h_A\frac{\xi_{3a1}\xi_9}{1+\xi_9} + h_B\frac{\xi_9}{p_{m1}+\xi_9} - \xi_{9a} - h_C\frac{\xi_{iap}\xi_{9a}}{p_{m6}+\xi_{9a}}$$

$$\frac{1}{k_{-8}}\frac{d\xi_3}{dt} = h_8 - p_{2a}\frac{\xi_{9a}\xi_3}{1+\xi_3} - p_{2b}\frac{\xi_{3a}\xi_3}{p_{m2b}+\xi_3} - p_{2c}\frac{\xi_p\xi_3}{p_{m2c}+\xi_3} - \xi_3$$

$$\frac{1}{k_{-5b}}\frac{d\xi_{3a}}{dt} = a_{2a}\frac{\xi_{9a}\xi_3}{1+\xi_3} + a_{2b}\frac{\xi_{3a}\xi_3}{p_{m2b}+\xi_3} + a_{2c}\frac{\xi_p\xi_3}{p_{m2c}+\xi_3} - a_5\frac{\xi_{iap}\xi_{3a}}{p_{m5}+\xi_{3a}} - \xi_{3a}$$

$$\frac{1}{k_{-4b}}\frac{d\xi_{iap}}{dt} = h_4 - p_{m4}\frac{\xi_{3a}\xi_{iap}}{1+\xi_{iap}} - \xi_{iap}$$

$$\frac{1}{k_{-3b}}\frac{d\xi_p}{dt} = h_3\xi_{pi} - p_{m3}\frac{\xi_{3a}\xi_p}{1+\xi_p} - \xi_p$$

$$\xi_{pi} = \xi_{ptot} - \xi_p$$

Supplementary material 3 – Dimensionless equations - Continued

Dimensionless Concentrations	Dimensionless Parameters
$\xi_9 = \frac{[C9]}{K_{m1a}}$	$h_7 = \frac{k_7}{k_{-7}K_{m1a}}$, $h_1 = \frac{k_{1a}}{k_{-7}}$
$\xi_{9a} = \frac{[C9_a]}{K_{m1a}}$	$h_{1b} = \frac{k_{1b}}{k_{-7}K_{m1a}}$, $p_{m1} = \frac{K_{m1b}}{K_{m1a}}$, $p_{m6} = \frac{K_{m-6b}}{K_{m1a}}$
$\xi_3 = \frac{[C3]}{K_{m2a}}$	$h_A = \frac{k_{1a}}{k_{-6a}}$, $h_B = \frac{k_{1b}}{k_{-6a}K_{m1a}}$, $h_C = \frac{k_{-6b}K_{m-4a}}{k_{-6a}K_{m1a}}$
$\xi_{3a} = \frac{[C3_a]}{K_{m2a}}$	$h_8 = \frac{k_8}{k_{-8}K_{m2a}}$, $p_{2a} = \frac{k_{2a}K_{m1a}}{k_{-8}K_{m2a}}$
$\xi_{3a1} = \frac{[C3_a]}{K_{m1a}}$	$p_{2b} = \frac{k_{2b}}{k_{-8}}$, $p_{2c} = \frac{k_{2c}K_{m-3a}}{k_{-8}K_{m2a}}$
$\xi_p = \frac{[PKC_a]}{K_{m-3a}}$	$p_{m2b} = \frac{K_{m2b}}{K_{m2a}}$, $p_{m2c} = \frac{K_{m2c}}{K_{m2a}}$
$\xi_{pi} = \frac{[PKC_i]}{K_{m-3a}}$	$a_{2a} = \frac{k_{2a}K_{m1a}}{k_{-5b}K_{m2a}}$, $a_{2b} = \frac{k_{2b}}{k_{-5b}}$, $a_{2c} = \frac{k_{2c}K_{m-3a}}{k_{-5b}K_{m2a}}$
$\xi_{ptot} = \frac{[PKC_{total}]}{K_{m-3a}}$	$a_5 = \frac{k_{-5a}K_{m-4a}}{k_{-5b}K_{m2a}}$, $p_{m5} = \frac{K_{m-5a}}{K_{m2a}}$
$\xi_{iap} = \frac{[IAP]}{K_{m-4a}}$	$h_4 = \frac{k_4}{k_{-4b}K_{m-4a}}$, $p_{m4} = \frac{k_{-4a}K_{m2a}}{k_{-4b}K_{m-4a}}$
	$h_3 = \frac{(k_{3a}[Api] + k_{3b})}{k_{-3b}}$, $p_{m3} = \frac{k_{-3a}K_{m2a}}{k_{-3b}K_{m-3a}}$

Equations of the model, rewritten to be dimensionless, the dimensionless concentrations, and dimensionless parameters.

Supplementary material 4 – Parameter values

Dimensionless parameter	Highest value used in simulation	Lowest value used in simulation	Literature value
h_7	50000	160	0.359712
h_1	1000	0.7	3.566667
h_{1b}	28000	20	0.06295
p_{m1}	0.42	0.1	---
h_A	100	0.035	3.566667
h_B	2800	1	---
h_C	210	0.005	1.00E+00
h_8	16000	0.571429	41.10997
p_{2a}	3170	0.057143	192.381
p_{2b}	244	2.28	101.9048
p_{2c}	7100	0.114286	---
p_{m2b}	10	0.1	0.4
p_{m2c}	10	0.1	---
p_{m6}	0.1	0.1	---
a_{2a}	3170	0.001	6.733333
a_{2b}	244	0.0399	3.566667
a_{2c}	7100	0.002	---
a_5	4100	0.001	0.4
p_{m5}	10	0.1	---
h_4	10000	4.666667	1.20E-01
p_{m4}	10	0.000667	1.486111
h_3	41000	0.091	---
p_{m3}	10000	0.092	1111.454

The values of the model's parameters were converted into corresponding dimensionless parameters. Comparison of the range of dimensionless parameters used in the simulations to the values of the dimensionless parameters based on the literature.

References

1. Simon, H. U.Apoptosis in Inflammatory Diseases. (1999) *Logo* **118**(2-4)
2. Friedlander, R. M.Apoptosis and Caspases in Neurodegenerative Diseases. (2003) *N Engl J Med* **348**(14), 1365-1375
3. Bennett, M. R. (2002) Apoptosis in the cardiovascular system. In. *Heart*, Br Cardiac Soc
4. Rupinder, S. K., Gurpreet, A. K., and Manjeet, S.Cell suicide and caspases. (2007) *Vascul Pharmacol* **46**(6), 383-393
5. Cohen, G. M.Caspases: the executioners of apoptosis. (1997) *Biochem J* **326**(Pt 1), 1-16
6. Degterev, A., Boyce, M., and Yuan, J.A decade of caspases. (2003) *Oncogene* **22**, 8543-8567
7. Doseff, A. I.Apoptosis: the sculptor of development. (2004) *Stem Cells Dev* **13**(5), 473-483
8. Walczak, H., and Haas, T. L.Biochemical analysis of the native TRAIL death-inducing signaling complex. (2008) *Methods Mol Biol* **414**, 221-239
9. Salvesen, G. S., and Duckett, C. S.IAP proteins: blocking the road to death's door. (2002) *Nat Rev Mol Cell Biol* **3**(6), 401-410
10. Thornberry, N. A., and Lazebnik, Y.Caspases: enemies within. (1998) *Science* **281**(5381), 1312-1316
11. Erhardt, P., and Cooper, G. M.Activation of the CPP32 Apoptotic Protease by Distinct Signaling Pathways with Differential Sensitivity to Bcl-x L. (2005) *J Biol Chem* **90**(2), 953-961
12. Kumar, S.Caspase function in programmed cell death. (2007) *Cell Death Differ* **14**, 32-43
13. Nicholson, D. W., Ali, A., Thornberry, N. A., Vaillancourt, J. P., Ding, C. K., Gallant, M., Gareau, Y., Griffin, P. R., Labelle, M., Lazebnik, Y. A., Munday, N. A., Raju, S. M., Smulson, M. E., Yamin, T.-T., Yu, V. L., and Miller, D. K.Identification and inhibition of the ICE/CED-3 protease necessary for mammalian apoptosis. (1995) *Nature* **376**(6535), 37
14. Slee, E. A., Harte, M. T., Kluck, R. M., Wolf, B. B., Casiano, C. A., Newmeyer, D. D., Wang, H. G., Reed, J. C., Nicholson, D. W., and Alnemri, E. S. (1999) Ordering the Cytochrome c-initiated Caspase Cascade: Hierarchical Activation of Caspases-2,-3,-6,-7,-8, and-10 in a Caspase-9-dependent Manner. In., Rockefeller Univ Press
15. Mittl, P. R. E., Di Marco, S., Krebs, J. F., Bai, X., Karanewsky, D. S., Priestle, J. P., Tomaselli, K. J., and Grutter, M. G.Structure of Recombinant Human CPP32 in Complex with the Tetrapeptide Acetyl-Asp-Val-Ala-Asp Fluoromethyl Ketone. (1997) *J. Biol. Chem.* **272**(10), 6539-6547
16. Slee, E. A., Adrain, C., and Martin, S. J.Executioner Caspase-3,-6, and-7 Perform Distinct, Non-redundant Roles during the Demolition Phase of Apoptosis. (2001) *J Biol Chem* **276**(10), 7320-7326
17. Fujita, E., Egashira, J., Urase, K., Kuida, K., and Momoi, T.Caspase-9 processing by caspase-3 via a feedback amplification loop in vivo.
18. Zou, H., Yang, R., Hao, J., Wang, J., Sun, C., Fesik, S. W., Wu, J. C., Tomaselli, K. J., and Armstrong, R. C.Regulation of the Apaf-1/Caspase-9 Apoptosome by Caspase-3 and XIAP. (2003) *J Biol Chem* **278**(10), 8091-8098
19. Borner, C.The Bcl-2 protein family: sensors and checkpoints for life-or-death decisions. (2003) *Mol Immunol* **39**(11), 615
20. Dean, E. J., Ranson, M., Blackhall, F., Holt, S. V., and Dive, C.Novel therapeutic targets in lung cancer: Inhibitor of apoptosis proteins from laboratory to clinic. (2007) *Cancer Treat Rev* **33**(2), 203-212
21. Suzuki, Y., Nakabayashi, Y., and Takahashi, R.Ubiquitin-protein ligase activity of X-linked inhibitor of apoptosis protein promotes proteasomal degradation of caspase-3 and enhances its anti-apoptotic effect in Fas-induced cell death. (2001) *Proc Natl Acad Sci U S A* **98**(15), 8662-8667
22. Deveraux, Q. L.Cleavage of human inhibitor of apoptosis protein XIAP results in fragments with distinct specificities for caspases. (1999) *EMBO J* **18**(19), 5242-5251
23. Voss, O. H., Batra, S., Kolattukudy, S. J., Gonzalez-Mejia, M., Smith, J. B., and Doseff, A. I.Binding of Caspase-3 Prodomain to Heat Shock Protein 27 Regulates Monocyte Apoptosis by Inhibiting Caspase-3 Proteolytic Activation. (2007) *J Biol Chem* **282**(34), 25088
24. Voss, O. H., Kim, S., Wewers, M. D., and Doseff, A. I.Regulation of Monocyte Apoptosis by the Protein Kinase C δ-dependent Phosphorylation of Caspase-3. (2005) *J Biol Chem* **280**(17), 17371-17379
25. Reyland, M. E.Protein kinase CÎ´ and apoptosis. (2007) *Biochem Soc Trans* **035**(5), 1001-1004
26. Malavez, Y., Gonzalez-Mejia, M.E., Doseff, A.I. (2008) PRKCD (protein kinase C, delta). In., Atlas Genet Cytogenet Oncol Haematol. http://atlasgeneticsoncology.org/Genes/GC_PRKCD.html, *in press.*
27. Ghayur, T., Hugunin, M., Talanian, R. V., Ratnofsky, S., Quinlan, C., Emoto, Y., Pandey, P., Datta, R., Huang, Y., Kharbanda, S., Allen, H., Kamen, R., Wong, W., and Kufe, D.Proteolytic Activation of

Protein Kinase C delta by an ICE/CED 3-like Protease Induces Characteristics of Apoptosis. (1996) *J. Exp. Med.* **184**(6), 2399-2404
28. Emoto, Y., Kisaki, H., Manome, Y., Kharbanda, S., and Kufe, D.Activation of protein kinase Cdelta in human myeloid leukemia cells treated with 1-beta-D-arabinofuranosylcytosine. (1996) *Blood* **87**(5), 1990
29. Mandil, R., Ashkenazi, E., Blass, M., Kronfeld, I., Kazimirsky, G., Rosenthal, G., Umansky, F., Lorenzo, P. S., Blumberg, P. M., and Brodie, C. (2001) Protein Kinase Ca and Protein Kinase Cd Play Opposite Roles in the Proliferation and Apoptosis of Glioma Cells 1. In. *Cancer Res*, AACR
30. Sumitomo, M., Ohba, M., Asakuma, J., Asano, T., Kuroki, T., Asano, T., and Hayakawa, M.Protein kinase Cd amplifies ceramide formation via mitochondrial signaling in prostate cancer cells. (2002) *J Clin Invest* **109**(6), 827-836
31. Way, T. D., Kao, M. C., and Lin, J. K.Apigenin Induces Apoptosis through Proteasomal Degradation of HER2/neu in HER2/neu-overexpressing Breast Cancer Cells via the Phosphatidylinositol 3-Kinase/Akt-dependent Pathway. (2004) *J Biol Chem* **279**(6), 4479-4489
32. Middleton Jr, E., Kandaswami, C., and Theoharides, T. C.The Effects of Plant Flavonoids on Mammalian Cells: Implications for Inflammation, Heart Disease, and Cancer. (2000) *Pharmacol Rev* **52**(4), 673
33. Stafford, H. A. (1990) *Flavonoid Metabolism*, CRC Press
34. Di Carlo, G., Mascolo, N., Izzo, A. A., and Capasso, F.Flavonoids: Old and new aspects of a class of natural therapeutic drugs. (1999) *Life Sci* **65**(4), 337-353
35. Middleton Jr, E.THE FLAVONOIDS AS POTENTIAL THERAPEUTIC AGENTS. (1996) *Immunopharmaceuticals*
36. Havsteen, B. H.The biochemistry and medical significance of the flavonoids. (2002) *Pharmacol Ther* **96**(2-3), 67-202
37. Vargo, M. A., Voss, O. H., Poustka, F., Cardounel, A. J., Grotewold, E., and Doseff, A. I.Apigenin-induced-apoptosis is mediated by the activation of PKCdelta and caspases in leukemia cells. (2006) *Biochem Pharmacol*
38. Wang, W., Heideman, L., Chung, C. S., Pelling, J. C., Koehler, K. J., and Birt, D. F.Cell-Cycle Arrest at G 2/M and Growth Inhibition by Apigenin in Human Colon Carcinoma Cell Lines. (2000) *Mol Carcinog* **28**(2), 102-110
39. Wang, I. K., Lin-Shiau, S. Y., and Lin, J. K.Induction of apoptosis by apigenin and related flavonoids through cytochrome c release and activation of caspase-9 and caspase-3 in leukaemia HL-60 cells. (1999) *Eur J Cancer* **35**(10), 1517-1525
40. Mak, P., Leung, Y., Tang, W., Harwood, C., and Ho, S. M.Apigenin suppresses cancer cell growth through ERbeta. (2006) *Neoplasia* **8**(11), 896-904
41. Shukla, S., and Gupta, S.Suppression of constitutive and tumor necrosis factor alpha-induced nuclear factor (NF)-kappaB activation and induction of apoptosis by apigenin in human prostate carcinoma PC-3 cells: correlation with down-regulation of NF-kappaB-responsive genes. (2004) *Clin Cancer Res* **10**(9), 3169-3178
42. Way, T. D., Kao, M. C., and Lin, J. K.Degradation of HER2/neu by apigenin induces apoptosis through cytochrome c release and caspase-3 activation in HER2/neu-overexpressing breast cancer cells. (2005) *FEBS Letters* **579**(1), 145-152
43. Morrissey, C., O'Neill, A., Spengler, B., Christoffel, V., Fitzpatrick, J. M., and Watson, R. W.Apigenin drives the production of reactive oxygen species and initiates a mitochondrial mediated cell death pathway in prostate epithelial cells. (2004) *Prostate* **63**(2), 131-142
44. Yin, F., Giuliano, A. E., Law, R. E., and Van Herle, A. J.Apigenin inhibits growth and induces G2/M arrest by modulating cyclin-CDK regulators and ERK MAP kinase activation in breast carcinoma cells. (2001) *Anticancer Res* **21**(1A), 413-420
45. Yang, L., Cao, Z., Yan, H., and Wood, W. C. (2003) Coexistence of High Levels of Apoptotic Signaling and Inhibitor of Apoptosis Proteins in Human Tumor Cells Implication for Cancer Specific Therapy 1. In. *Cancer Res*, AACR
46. Morse-Gaudio, M., Connolly, J. M., and Rose, D. P.Protein kinase C and its isoforms in human breast cancer cells: relationship to the invasive phenotype. (1998) *Int J Oncol* **12**(6), 1349-1354
47. Lu, Z., Hornia, A., Jiang, Y. W., Zang, Q., Ohno, S., and Foster, D. A.Tumor promotion by depleting cells of protein kinase C delta. (1997) *Mol Cell Biol* **17**(6), 3418-3428
48. Sitailo, L. A., Tibudan, S. S., and Denning, M. F.Activation of Caspase-9 Is Required for UV-induced Apoptosis of Human Keratinocytes. (2002) *J. Biol. Chem.* **277**(22), 19346-19352
49. Legewie, S., Blüthgen, N., and Herzel, H.Mathematical Modeling Identifies Inhibitors of Apoptosis as Mediators of Positive Feedback and Bistability. (2006) *PLoS Comput Biol* **2**(9), e120

50. Li, C., and Wong, W. H.Model-based analysis of oligonucleotide arrays: Expression index computation and outlier detection. (2001) *Proc Natl Acad Sci U S A* **98**(1), 31
51. Kanehisa, M., Araki, M., Goto, S., Hattori, M., Hirakawa, M., Itoh, M., Katayama, T., Kawashima, S., Okuda, S., Tokimatsu, T., and Yamanishi, Y.KEGG for linking genomes to life and the environment. (2008) *Nucl. Acids Res.* **36**(suppl_1), D480-484
52. Kanehisa, M., Goto, S., Hattori, M., Aoki-Kinoshita, K. F., Itoh, M., Kawashima, S., Katayama, T., Araki, M., and Hirakawa, M.From genomics to chemical genomics: new developments in KEGG. (2006) *Nucl. Acids Res.* **34**(suppl_1), D354-357
53. Kanehisa, M., and Goto, S.KEGG: Kyoto Encyclopedia of Genes and Genomes. (2000) *Nucl. Acids Res.* **28**(1), 27-30
54. Salomonis, N., Hanspers, K., Zambon, A. C., Vranizan, K., Lawlor, S. C., Dahlquist, K. D., Doniger, S. W., Stuart, J., Conklin, B. R., and Pico, A. R.GenMAPP 2: new features and resources for pathway analysis. (2007) *BMC Bioinformatics* **8**, 217
55. Ashburner, M., Ball, C. A., Blake, J. A., Botstein, D., Butler, H., Cherry, J. M., Davis, A. P., Dolinski, K., Dwight, S. S., and Eppig, J. T.Gene Ontology: tool for the unification of biology. (2000) *Nat Genet* **25**, 25-29
56. Songyang, Z., Blechner, S., Hoagland, N., Hoekstra, M. F., Piwnica-Worms, H., and Cantley, L. C.Use of an oriented peptide library to determine the optimal substrates of protein kinases. (1994) *Curr Biol* **4**(11), 973
57. Blom, N., Gammeltoft, S., and Brunak, S.Sequence and structure-based prediction of eukaryotic protein phosphorylation sites. (1999) *J Mol Biol* **294**(5), 1351-1362
58. Blom, N., Sicheritz-Ponten, T., Gupta, R., Gammeltoft, S., and Brunak, S.Prediction of post-translational glycosylation and phosphorylation of proteins from the amino acid sequence. (2004) *Proteomics* **4**(6), 1633-1649
59. Xue, Y., Zhou, F., Zhu, M., Ahmed, K., Chen, G., and Yao, X.GPS: a comprehensive www server for phosphorylation sites prediction. (2005) *Nucl. Acids Res.* **33**(suppl_2), W184-187
60. Zhou, F.-F., Xue, Y., Chen, G.-L., and Yao, X.GPS: a novel group-based phosphorylation predicting and scoring method. (2004) *Biochem Biophys Res Commun* **325**(4), 1443
61. Arnold, K., Bordoli, L., Kopp, J., and Schwede, T.The SWISS-MODEL workspace: a web-based environment for protein structure homology modelling. (2006) *Bioinformatics* **22**(2), 195-201
62. Kopp, J., and Schwede, T.The SWISS-MODEL Repository of annotated three-dimensional protein structure homology models. *Nucl. Acids Res.*
63. Schwede, T., Kopp, J., Guex, N., and Peitsch, M. C.SWISS-MODEL: an automated protein homology-modeling server. (2003) *Nucleic Acids Res* **31**(13), 3381-3385
64. Guex, N., and Peitsch, M. C.SWISS-MODEL and the Swiss-PdbViewer: an environment for comparative protein modeling. (1997) *Electrophoresis* **18**(15), 2714-2723
65. Peitsch, M. C.Protein Modeling by E-mail. (1995) *Bio/Technology* **13**(7), 658-660
66. DeLano, W. L. (2002) The PyMOL Molecular Graphics System. In., DeLano Scientific, Palo Alto, CA
67. Cheong, R., and Levchenko, A.Wires in the soup: quantitative models of cell signaling. (2008) *Trends Cell Biol* **18**(3), 112
68. Aksan, I., and Kurnaz, M. L.A Computer-Based Model for the Regulation of Mitogen Activated Protein Kinase (MAPK) Activation. (2003) *J Recept Signal Transduct* **23**(2), 197-209
69. Han, Z., Hendrickson, E. A., Bremner, T. A., and Wyche, J. H.A Sequential Two-Step Mechanism for the Production of the Mature p17: p12 Form of Caspase-3 in Vitro. (1997) *J Biol Chem* **272**(20), 13432-13436
70. DeVita Jr, V. T., Young, R. C., and Canellos, G. P.Combination versus single agent chemotherapy: a review of the basis for selection of drug treatment of cancer. (1975) *Cancer* **35**(1), 98-110
71. Begbie, S. D., Kerestes, Z. L., and Bell, D. R.Patterns of alternative medicine use by cancer patients. (1996) *Med J Aust* **165**(10), 545-548
72. Sun, X. M., MacFarlane, M., Zhuang, J., Wolf, B. B., Green, D. R., and Cohen, G. M.Distinct Caspase Cascades Are Initiated in Receptor-mediated and Chemical-induced Apoptosis. (1999) *J Biol Chem* **274**(8), 5053-5060
73. Yoo, N., Kim, H., Kim, S. U. Y., Park, W., Kim, S. H. O., Lee, J. Y., and Lee, S.Stomach cancer highly expresses both initiator and effector caspases; an immunohistochemical study. (2002) *Apmis* **110**(11), 825-832
74. Varterasian, M. L., Mohammad, R. M., Shurafa, M. S., Hulburd, K., Pemberton, P. A., Rodriguez, D. H., Spadoni, V., Eilender, D. S., Murgo, A., and Wall, N. (2000) Phase II Trial of Bryostatin 1 in Patients with Relapsed Low-Grade Non-Hodgkin's Lymphoma and Chronic Lymphocytic Leukemia 1. In. *Clin Cancer Res*, AACR

75. Middleton, E., and Kandaswami, C.Effects of flavonoids on immune and inflammatory cell functions. (1992) *Biochem Pharmacol* **43**(6), 1167-1179
76. MojŠIlovÊ, G., and Kuchta, M.Dietary Flavonoids and Risk of Coronary Heart Disease. (2001) *Physiol. Res* **50**, 529-535
77. Lim, H., and Kim, H. P.Inhibition of Mammalian Collagenase, Matrix Metalloproteinase-1, by Naturally-Occurring Flavonoids. (2007) *Planta Med* **73**, 1267-1274
78. Kim, E. K., Kwon, K., Song, M. Y., Han, M. J., Lee, J. H., Lee, Y., Lee, J. H., Ryu, D., Park, B. H., and Park, J. W.Flavonoids Protect Against Cytokine-Induced Pancreatic [beta]-Cell Damage Through Suppression of Nuclear Factor [kappa] B Activation. (2007) *Pancreas* **35**(4), e1-e9
79. Nicholas, C., Batra, S., Vargo, M. A., Voss, O. H., Gavrilin, M. A., Wewers, M. D., Guttridge, D. C., Grotewold, E., and Doseff, A. I.Apigenin Blocks Lipopolysaccharide-Induced Lethality In Vivo and Proinflammatory Cytokines Expression by Inactivating NF-κB through the Suppression of p65 Phosphorylation. (2007) *The Journal of Immunology* **179**(10), 7121
80. Shukla, S., MacLennan, G. T., Flask, C. A., Fu, P., Mishra, A., Resnick, M. I., and Gupta, S.Blockade of β-Catenin Signaling by Plant Flavonoid Apigenin Suppresses Prostate Carcinogenesis in TRAMP Mice. (2007) *Cancer Res* **67**(14), 6925
81. Giraud, S., Bienvenu, F., Avril, S., Gascan, H., Heery, D. M., and Coqueret, O.Functional Interaction of STAT3 Transcription Factor with the Coactivator NcoA/SRC1a. (2002) *J. Biol. Chem.* **277**(10), 8004-8011
82. Her, C., Zhao, N., Wu, X., and Tompkins, J. D.MutS homologues hMSH4 and hMSH5: diverse functional implications in humans. (2007) *Front Biosci* **12**, 905-911
83. Cho, S., Ko, H. M., Kim, J. M., Lee, J. A., Park, J. E., Jang, M. S., Park, S. G., Lee, D. H., Ryu, S. E., and Park, B. C.Positive Regulation of Apoptosis Signal-regulating Kinase 1 by hD53L1. (2004) *J Biol Chem* **279**(16), 16050-16056
84. Hemmati, P. G., Gillissen, B., von Haefen, C., Wendt, J., Stärck, L., Güner, D., Dörken, B., and Daniel, P. T.Adenovirus-mediated overexpression of p14 ARF induces p53 and Bax-independent apoptosis. (2002) *Oncogene* **21**, 3149-3161
85. Marani, M., Tenev, T., Hancock, D., Downward, J., and Lemoine, N. R.Identification of Novel Isoforms of the BH3 Domain Protein Bim Which Directly Activate Bax To Trigger Apoptosis. (2002) *Mol. Cell. Biol.* **22**(11), 3577-3589
86. Ohshima, H., Tatemichi, M., and Sawa, T.Chemical basis of inflammation-induced carcinogenesis. (2003) *Arch Biochem Biophys* **417**(1), 3-11
87. Farrow, B., and Evers, B. M.Inflammation and the development of pancreatic cancer. (2002) *Surg Oncol* **10**(4), 153-169
88. Wisdom, R., Johnson, R. S., and Moore, C.c-Jun regulates cell cycle progression and apoptosis by distinct mechanisms. (1999) *EMBO J* **18**, 188-197
89. McDonald, D. R., Janssen, R., and Geha, R.Lessons learned from molecular defects in nuclear factor?B dependent signaling. (2006) *Microbes Infect* **8**(4), 1151-1156
90. Wang, R. F., Miyahara, Y., and Wang, H. Y.Toll-like receptors and immune regulation: implications for cancer therapy. *Oncogene* **27**(2), 181
91. Lee, N. K., and Lee, S. Y.Modulation of life and death by the tumor necrosis factor receptor-associated factors (TRAFs). (2002) *J Biochem Mol Biol* **35**(1), 61-66
92. Takaoka, A., Yanai, H., Kondo, S., Duncan, G., Negishi, H., Mizutani, T., Kano, S., Honda, K., Ohba, Y., and Mak, T. W.Integral role of IRF-5 in the gene induction programme activated by Toll-like receptors. (2005) *Nature* **434**(7030), 243-249
93. Zhang, T., Guo, C.-J., Li, Y., Douglas, S. D., Qi, X.-X., Song, L., and Ho, W.-Z.Interleukin-1[beta] induces macrophage inflammatory protein-1[beta] expression in human hepatocytes. (2003) *Cell Immunol* **226**(1), 45
94. Pahl, H. L.Activators and target genes of Rel/NF-kappa B transcription factors.
95. Barnes, B. J., Richards, J., Mancl, M., Hanash, S., Beretta, L., and Pitha, P. M.Global and Distinct Targets of IRF-5 and IRF-7 during Innate Response to Viral Infection. (2004) *J. Biol. Chem.* **279**(43), 45194-45207
96. Harris, R. E.Cyclooxygenase-2 (COX-2) and the Inflammogenesis of Cancer. *Inflammation in the Pathogenesis of Chronic Diseases* **42**, 93–126
97. Nagata, S.Apoptosis by death factor. (1997) *Apoptosis* **88**, 355-365
98. Imai, Y., Kimura, T., Murakami, A., Yajima, N., Sakamaki, K., and Yonehara, S.The CED-4-homologous protein FLASH is involved in Fas-mediated activation of caspase-8 during apoptosis. (1999) *Nature* **398**, 777-785
99. Koonin, E. V., Aravind, L., Hofmann, K., Tschopp, J., and Dixit, V. M.Apoptosis: Searching for FLASH domains. (1999) *Nature* **401**(6754), 662

100. Lakshmanan, U., and Porter, A. G.Caspase-4 Interacts with TNF Receptor-Associated Factor 6 and Mediates Lipopolysaccharide-Induced NF-κB-Dependent Production of IL-8 and CC Chemokine Ligand 4 (Macrophage-Inflammatory Protein-1). (2007) *The Journal of Immunology* **179**(12), 8480
101. Stang, M. T., Armstrong, M. J., Watson, G. A., Sung, K. Y., Liu, Y., Ren, B., and Yim, J. H.Interferon regulatory factor-1-induced apoptosis mediated by a ligand-independent fas-associated death domain pathway in breast cancer cells. (2007) *Oncogene* **4**
102. Au, P. Y., and Yeh, W. C.Physiological roles and mechanisms of signaling by TRAF2 and TRAF5. (2007) *Adv Exp Med Biol* **597**, 32-47
103. Trendelenburg, G.Acute neurodegeneration and the inflammasome: central processor for danger signals and the inflammatory response? (2008) *J Cereb Blood Flow Metab*
104. Keating, S. E., Maloney, G. M., Moran, E. M., and Bowie, A. G.IRAK-2 Participates in Multiple Toll-like Receptor Signaling Pathways to NFκB via Activation of TRAF6 Ubiquitination. (2007) *J. Biol. Chem.* **282**(46), 33435-33443
105. Temkin, V., and Karin, M.From death receptor to reactive oxygen species and c-Jun N-terminal protein kinase: the receptor-interacting protein 1 odyssey. (2007) *Immunol Rev* **220**(1), 8-21
106. Rouault, J.-P., Falette, N., Guehenneux, F., Guillot, C., Rimokh, R., Wang, Q., Berthet, C., Moyret-Lalle, C., Savatier, P., Pain, B., Shaw, P., Berger, R., Samarut, J., Magaud, J.-P., Ozturk, M., Samarut, C., and Puisieux, A.Identification of BTG2, an antiproliferative p53-dependent component of the DNA damage cellular response pathway. (1996) *Nat Genet* **14**(4), 482
107. Mansky, K. C., Sankar, U., Han, J., and Ostrowski, M. C.Microphthalmia Transcription Factor Is a Target of the p38 MAPK Pathway in Response to Receptor Activator of NF-kappa B Ligand Signaling. (2002) *J. Biol. Chem.* **277**(13), 11077-11083
108. Yang, B. S., Hauser, C. A., Henkel, G., Colman, M. S., Van Beveren, C., Stacey, K. J., Hume, D. A., Maki, R. A., and Ostrowski, M. C.Ras-mediated phosphorylation of a conserved threonine residue enhances the transactivation activities of c-Ets1 and c-Ets2. (1996) *Mol. Cell. Biol.* **16**(2), 538-547
109. Kim, M. K., Kang, M. R., Nam, H. W., Bae, Y.-S., Kim, Y. S., and Chung, I. K.Regulation of telomeric-repeat binding factor 1 binding to telomeres by casein kinase 2-mediated phosphorylation. (2008) *J. Biol. Chem.*, M710065200
110. Kass, E. M., Ahn, J., Tanaka, T., Freed-Pastor, W. A., Keezer, S., and Prives, C.Stability of Checkpoint Kinase 2 Is Regulated via Phosphorylation at Serine 456. (2007) *J. Biol. Chem.* **282**(41), 30311-30321
111. Ganesan, R., Mittl, P. R. E., Jelakovic, S., and Grütter, M. G.Extended Substrate Recognition in Caspase-3 Revealed by High Resolution X-ray Structure Analysis. (2006) *J Mol Biol* **359**(5), 1378-1388
112. Allan, L. A., Morrice, N., Brady, S., Magee, G., Pathak, S., and Clarke, P. R.Inhibition of caspase-9 through phosphorylation at Thr 125 by ERK MAPK. (2003) *Nat Cell Biol* **5**(7), 647-654
113. Alvarado-Kristensson, M., Melander, F., Leandersson, K., Ronnstrand, L., Wernstedt, C., and Andersson, T.p38-MAPK Signals Survival by Phosphorylation of Caspase-8 and Caspase-3 in Human Neutrophils Abbreviations used in this paper: AMC, aminomethylcoumarin; IPTG, isopropyl-1-thio-ß-d-galactopyranoside; MAPK, mitogen-activated protein kinase. (2004) *J Exp Med* **199**(4), 449-458
114. Roy, S., Bayly, C. I., Gareau, Y., Houtzager, V. M., Kargman, S., Keen, S. L. C., Rowland, K., Seiden, I. M., Thornberry, N. A., and Nicholson, D. W.Maintenance of caspase-3 proenzyme dormancy by an intrinsic" safety catch" regulatory tripeptide. (2001) *Proc Natl Acad Sci U S A* **98**(11), 6132
115. Kang, S.-J., Wang, S., Hara, H., Peterson, E. P., Namura, S., Amin-Hanjani, S., Huang, Z., Srinivasan, A., Tomaselli, K. J., Thornberry, N. A., Moskowitz, M. A., and Yuan, J.Dual Role of Caspase-11 in Mediating Activation of Caspase-1 and Caspase-3 Under Pathological Conditions. (2000) *J. Cell Biol.* **149**(3), 613-622
116. Gygi, S. P., Rochon, Y., Franza, B. R., and Aebersold, R.Correlation between Protein and mRNA Abundance in Yeast. (1999) *Mol. Cell. Biol.* **19**(3), 1720-1730
117. Fahy, R. J., Doseff, A. I., and Wewers, M. D.Spontaneous Human Monocyte Apoptosis Utilizes a Caspase-3-Dependent Pathway That Is Blocked by Endotoxin and Is Independent of Caspase-1. (1999) *J Immunol* **163**(4), 1755-1762
118. Bentele, M., Lavrik, I., Ulrich, M., Stosser, S., Heermann, D. W., Kalthoff, H., Krammer, P. H., and Eils, R.Mathematical modeling reveals threshold mechanism in CD95-induced apoptosis M. Bentele and I. Lavrik contributed equally to this work. Abbreviations used in this paper: CHX, cyclohexamide; DD, death domain; DISC, death-inducing signaling complex. (2004) *J Cell Biol* **166**(6), 839-851
119. Yin, Q., Park, H. H., Chung, J. Y., Lin, S. C., Lo, Y. C., da Graca, L. S., Jiang, X., and Wu, H.Caspase-9 holoenzyme is a specific and optimal procaspase-3 processing machine. (2006) *Mol Cell* **22**(2), 259-268
120. Woodgett, J. R., and Hunter, T.Immunological evidence for two physiological forms of protein kinase C. (1987) *Mol Cell Biol* **7**(1), 85-96

121. Bagci, E. Z., Vodovotz, Y., Billiar, T. R., Ermentrout, G. B., and Bahar, I.Bistability in Apoptosis: Roles of Bax, Bcl-2, and Mitochondrial Permeability Transition Pores. (2006) *Biophys J* **90**(5), 1546-1559
122. Tan, M., Gallegos, J. R., Gu, Q., Huang, Y., Li, J., Jin, Y., Lu, H., and Sun, Y.SAG/ROC-SCF ß-TrCP E3 Ubiquitin Ligase Promotes Pro-Caspase-3 Degradation as a Mechanism of Apoptosis Protection. (2006) *Neoplasia* **8**(12), 1042-1054
123. Barcaroli, D., Dinsdale, D., Neale, M. H., Bongiorno-Borbone, L., Ranalli, M., Munarriz, E., Sayan, A. E., McWilliam, J. M., Smith, T. M., and Fava, E.FLASH is an essential component of Cajal bodies. (2006) *Proc Natl Acad Sci US A* **103**(40), 14802
124. Kino, T., and Chrousos, G. P.Tumor Necrosis Factor a Receptor-and Fas-associated FLASH Inhibit Transcriptional Activity of the Glucocorticoid Receptor by Binding to and Interfering with Its Interaction with p160 Type Nuclear Receptor Coactivators. (2003) *J Biol Chem* **278**(5), 3023-3029
125. Du, X., Tang, W., Tian, W., Li, S., Li, X., Liu, L., Zheng, X., Chen, X., Lin, Y., and Tang, Y.Novel IRF6 Mutations in Chinese Patients with Van der Woude Syndrome. (2006) *J Dent Res* **85**(10), 937
126. Wang, Z., Zhang, B., Yang, L., Ding, J., and Ding, H. F.Constitutive production of NF-kappa B2 p52 is not tumorigenic but predisposes mice to inflammatory autoimmune disease by repressing Bim expression. (2008) *J Biol Chem*
127. Oh S., P. L. P., Terabe M., Ni L., Waldmann T.A., Berzofsky J.A.Il-15 as a mediator of CD4+ help for CD8+ T cell longevity and avoidance of TRAIL-mediated apoptosis. (2008) *Proc Natl Acad Sci US A* **105**(13), 5201-5206
128. Kristjansdottir, G., Sandling, J. K., Bonetti, A., Roos, I. M., Milani, L., Wang, C., Gustafsdottir, S. M., Sigurdsson, S., Lundmark, A., and Tienari, P. J.Interferon Regulatory Factor 5 (IRF5) Gene Variants are Associated with Multiple Sclerosis in Three Distinct Populations. (2008) *J Med Genet*
129. Couzinet, A., Tamura, K., Chen, H., Nishimura, K., Wang, Z. C., Morishita, Y., Takeda, K., Yagita, H., Yanai, H., and Taniguchi, T.A cell-type-specific requirement for IFN regulatory factor 5 (IRF5) in Fas-induced apoptosis. (2008) *Proc Natl Acad Sci U S A* **105**(7), 2556
130. Ishida, T. K., Tojo, T., Aoki, T., Kobayashi, N., Ohishi, T., Watanabe, T., Yamamoto, T., and Inoue, J.TRAF5, a novel tumor necrosis factor receptor-associated factor family protein, mediates CD40 signaling. (1996) *Proc Natl Acad Sci US A* **93**(18), 9437-9442
131. Dai, W. B., Zheng, Y. W., Mi, X. Y., Liu, N., Lin, H., and Yan, J.Expression and Significance of TRAF4 Protein in Breast Carcinoma. (1910) *Ai Zheng* **2007**, 1095-1098
132. Barbaric, D., Byth, K., Dalla-Pozza, L., and Byrne, J. A.Expression of tumor protein D52-like genes in childhood leukemia at diagnosis: Clinical and sample considerations. (2006) *Leuk Res* **30**(11), 1355-1363
133. Boutros, R., and Byrne, J. A.D53 (TPD52L1) is a cell cycle-regulated protein maximally expressed at the G2-M transition in breast cancer cells. (2005) *Exp Cell Res* **310**(1), 152-165
134. Eckhart, L., Kittel, C., Gawlas, S., Gruber, F., Mildner, M., Jilma, B., and Tschachler, E.Identification of a novel exon encoding the amino-terminus of the predominant caspase-5 variants. (2006) *Biochem Biophys Res Commun* **348**(2), 682-688
135. Ringwood, L., and Li, L.The involvement of the interleukin-1 receptor-associated kinases (IRAKs) in cellular signaling networks controlling inflammation. (2008) *Cytokine*
136. Tsujimoto, H., Ono, S., Efron, P. A., Scumpia, P. O., Moldawer, L. L., and Mochizuki, H.ROLE OF TOLL-LIKE RECEPTORS IN THE DEVELOPMENT OF SEPSIS.
137. Silva, T. A., Leite Ribeiro, F. L., De Oliveira-Neto, H. H., Watanabe, S., De Cassia Goncalves Alencar, R., Fukada, S. Y., Queiroz Cunha, F., Rodrigues Leles, C., Mendonca, E. F., and Carvalho Batista, A.Dual role of CCL3/CCR1 in oral squamous cell carcinoma: Implications in tumor metastasis and local host defense. (2007) *Oncol Rep* **18**(5), 1107-1113
138. Menten, P., Wuyts, A., and Van Damme, J.Macrophage inflammatory protein-1. (2002) *Cytokine Growth Factor Rev* **13**(6), 455
139. Ryter, S. W., Alam, J., and Choi, A. M. K.Heme Oxygenase-1/Carbon Monoxide: From Basic Science to Therapeutic Applications. (2006) *Physiol Rev* **86**(2), 583-650
140. Boiko, A. D., Porteous, S., Razorenova, O. V., Krivokrysenko, V. I., Williams, B. R., and Gudkov, A. V.A systematic search for downstream mediators of tumor suppressor function of p53 reveals a major role of BTG2 in suppression of Ras-induced transformation. (2006) *Genes Dev.* **20**(2), 236-252
141. Guardavaccaro, D., Corrente, G., Covone, F., Micheli, L., D'Agnano, I., Starace, G., Caruso, M., and Tirone, F.Arrest of G1-S Progression by the p53-Inducible Gene PC3 Is Rb Dependent and Relies on the Inhibition of Cyclin D1 Transcription. (2000) *Mol. Cell. Biol.* **20**(5), 1797-1815
142. Vega, H., Waisfisz, Q., Gordillo, M., Sakai, N., Yanagihara, I., Yamada, M., van Gosliga, D., Kayserili, H., Xu, C., Ozono, K., Wang Jabs, E., Inui, K., and Joenje, H.Roberts syndrome is caused by

mutations in ESCO2, a human homolog of yeast ECO1 that is essential for the establishment of sister chromatid cohesion. (2005) *Nat Genet* **37**(5), 468